Carlin-type geochemical signal in lake and stream sediments from the Kechika trough, north-central British Columbia

Alexei S. Rukhlov[1, a], Tian Han[1], JoAnne Nelson[1], Adrian S. Hickin[1], and Filippo Ferri[2]

[1] British Columbia Geological Survey, Ministry of Energy and Mines, Victoria, BC, V8W 9N3
[2] Ministry of Natural Gas Development, 1810 Blanshard Street, Victoria, BC, V8W 9N3
[a] corresponding author: Alexei.Rukhlov@gov.bc.ca

Recommended citation: Rukhlov, A.S., Han, T., Nelson, J., Hickin, A.S., and Ferri, F., 2015. Carlin-type geochemical signal in lake and stream sediments from the Kechika trough, north-central British Columbia. In: Geological Fieldwork 2014, British Columbia Ministry of Energy and Mines, British Columbia Geological Survey Paper 2015-1, pp. 165-188.

Abstract
Statistically robust treatment of multi-element geochemical data using simultaneous regression analysis, principal components analysis, and weighted sum indices can reveal economically significant anomalies that might otherwise be masked. Robust analysis of data from the National Geochemical Reconnaissance and the Regional Geochemical Survey programs document Au±As±Hg±Tl±Sb enrichment in stream and lake sediments from the Kechika trough, a long-lived (Neoproterozoic to Paleozoic) deep-water basin in north-central British Columbia. A similar enrichment is found in stream sediments sourced from recently discovered Carlin-type gold and realgar occurrences in Selwyn basin, the northward continuation of Kechika trough in the Rackla belt of east-central Yukon. In both areas, anomalous values are spatially related to platform to deep-water basin transitions and to extensional structures that originated during basin subsidence and then reactivated as thrusts during regional shortening. These anomalies and geologic setting are comparable to those of Carlin-type gold deposits of the Great Basin in Nevada. The Kechika trough may hold potential for Carlin-type deposits.

Keywords: Kechika trough, Selwyn basin, Carlin-type, Regional Geochemical Survey, stream- and lake-sediment geochemistry

1. Introduction

Eocene Carlin-type gold deposits (CTGD's) of the Great Basin in Nevada are some of the most prolific in the world (Muntean et al., 2011). In these deposits, gold occurs primarily in fine-grained (1-5 µm) arsenian pyrite and as µm-sized particles disseminated in quartz that are hosted by Paleozoic silty carbonate and siliceous sedimentary rocks altered by decarbonatization, silicification (jasperoid) and argillization processes. Enrichment in As-Hg-Tl-Sb±Te reflects realgar, orpiment, and stibnite in late-stage calcite veins that locally contain barite. Controlled both by stratigraphy and structure, the Carlin deposits have notably low Ag and base metal contents relative to spatially associated Paleozoic sedimentary exhalite (SEDEX) and Mesozoic to Cenozoic intrusion-related deposits. A widely accepted genetic model for CTGDs is lacking; both magmas and crust have been proposed as sources for auriferous fluids. Nonetheless, the Carlin deposits appear to mark intense hydrothermal activity from renewed magmatism in Great Basin between 42 and 34 Ma, during a change from regional shortening to extension (Arehart, 1996; Muntean et al., 2011).

Gold and realgar showings with similar stratigraphic and structural controls have recently been discovered in Proterozoic to Paleozoic strata of Selwyn basin in the Rackla belt, east-central Yukon (Fig. 1; ATAC Resources Ltd., 2010; Arehart et al., 2013; Tucker et al., 2013). These discoveries raise the possibility of similar occurrences in the Kechika trough, the southward continuation of Selwyn basin in north-central British Columbia (Fig. 1; Poulsen, 1996). This study evaluates multi-element stream- and lake-sediment geochemical data to test the Carlin-type potential of the Kechika trough. These data were generated by the National Geochemical Reconnaissance (NGR; Friske et al., 1991a, b; Héon, 2003; Day et al., 2009; Jackaman, 2011b) and Regional Geochemical Survey (RGS; Jackaman et al., 1996; Lett et al., 1996; Cook et al., 1997, 1999; Jackaman, 2011a) programs. Our robust statistical treatment, which is validated by identifying geochemical signatures at known Carlin-type showings in the Rackla belt, highlights similar geochemical anomalies in the Kechika trough, suggesting that it holds potential for similar deposits.

2. Regional setting

2.1. Kechika trough

The Kechika trough, in the Foreland Fold and Thrust belt of the northern Canadian Cordillera, is a long-lived, deep-water basin that formed between the MacDonald platform to the east and the Cassiar platform to the west (Fig. 1; Gabrielse, 1962; 1963a, b; 1998; Ferri et al., 1999). Northward it connects to, and shares stratigraphic and structural elements with, the Selwyn basin in Yukon Territory (Fig. 1). The Kechika trough was filled with fine-grained, deep-water deposits that are equivalent to platform strata to the east. The oldest rocks in the basin include Neoproterozoic rift-related siliciclastic rocks (Hyland Group and Gataga volcanic rocks). The youngest strata consist of Cenozoic conglomerates, sandstones, and mafic volcanic rocks. Most of the study area is underlain by Cambrian to early

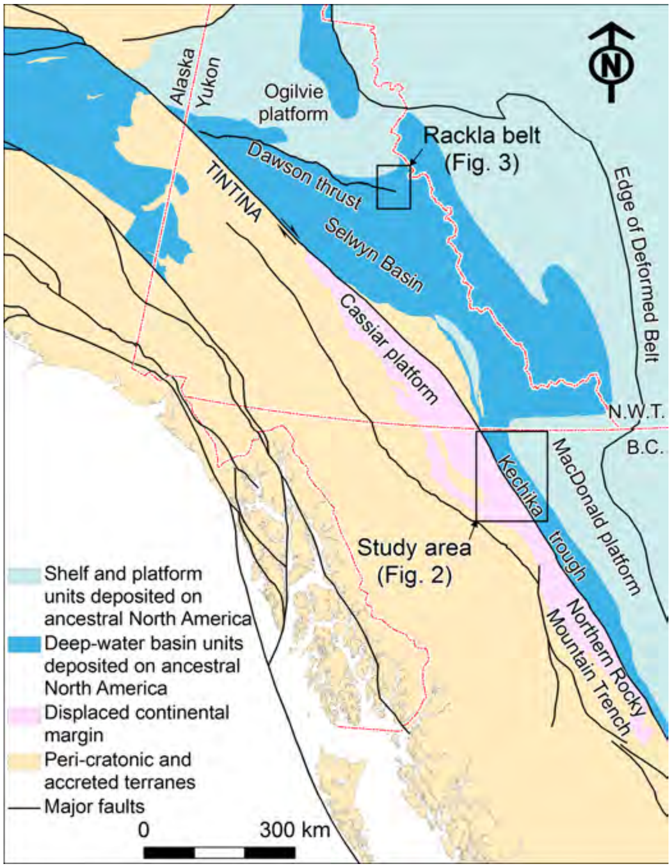

Fig. 1. Simplified geology and locations of Kechika trough study area in north-central British Columbia and the Rackla belt of Carlin-type Au mineralization in east-central Yukon.

Mississippian fine-grained siliciclastic and carbonate rocks (Gog, Kechika, Road River and Earn groups). Minor intrusive rocks include Early Paleozoic mafic sills and dikes and small Early Cretaceous to Eocene (?) granitic feldspar porphyry stocks, dikes and sills (Fig. 2).

Transitions from platform to deep-water sedimentation were probably controlled by syndepositional growth faults. Episodes of extension during the Paleozoic terminated at the end of the early Jurassic with the onset of compressional tectonics, which generated the predominantly easterly vergent thrusts and folds that characterize the northern Rocky Mountains. Some thrusts appear to be reactivated growth faults. For example, eruption of the Gataga volcanic rocks (ca. 690 Ma) was localized along a syndepositional fault; reactivated slip with a reverse sense during Jura-Cretaceous thrusting juxtaposed these rocks against strata as young as Devonian (Ferri et al., 1999).

SEDEX barite±sulphide mineralization is the most important mineral deposit type in the Kechika trough. These stratiform Zn-Pb-Ag-Ba deposits are in Cambrian, Middle Ordovician, Lower Silurian, and Upper Devonian strata (Fig. 2). The most significant are hosted by Upper Devonian shales, cherts, and slates in the lower part of the Earn Group. These include the Cirque (Stronsay), Driftpile Creek, Akie, Bear and Mount Alcock deposits. The trough also contains porphyry and skarn W-Mo±Cu mineralization related to early Cretaceous intrusions (e.g., Boya showings) and sulphide vein Ag-Pb-Zn-Cu mineralization (Ferri et al., 1999).

2.2. Rackla belt

The Rackla belt is on the northern edge of Selwyn basin (Fig. 1). Most of the area is underlain by deep-water basin to shelf and slope strata. They consist of fine-grained siliciclastic and carbonate rocks, ranging from Neoproterozoic (Yusezyu, Algae, and Narchilla formations of the Hyland Group) to Devonian-Mississippian (Earn Group) and locally Carboniferous to Triassic strata (Fig. 3). Cambrian to Devonian platformal carbonate rocks overlie the Neoproterozoic strata north of the long-lived Dawson thrust zone and the Kathleen Lakes fault (Chakungal and Bennett, 2011; Colpron et al., 2013). Late Cretaceous and Paleocene felsic intrusions occur throughout Selwyn basin to the west and south of the area (Hart et al., 2004; Thiessen et al., 2012).

Similar to the Kechika trough, platform to deep-water basin transitions in the Rackla belt were controlled by syndepositional structures, as indicated by significant changes in thickness of Neoproterozoic strata across north-trending faults. Changes in Neoproterozoic to Paleozoic stratigraphy across the Dawson and Kathleen Lakes faults suggest fault reactivation in the Paleozoic, and during Mesozoic folding and thrusting (Colpron et al., 2013).

Long-lived faults, combined with favourable carbonate host strata at the shelf-slope transition, localized mineralization. Neoproterozoic fine-grained siliciclastic and carbonate rocks host most of the Carlin-type gold and realgar mineralization discovered to date (Osiris, Isis, Conrad and Pharoah zones; ATAC Resources Ltd., 2010; Arehart et al., 2013). The Carlin-type mineralization is spatially associated with Mississippi Valley-type Ag-Pb-Zn occurrences hosted by both Proterozoic and Paleozoic carbonate rocks (Chakungal and Bennett, 2011). The Earn Group (Devonian-Mississippian) controls SEDEX and volcanogenic massive sulphide (VMS) barite and Pb-Zn-Ag±Cu occurrences (e.g., Marg deposit). Nearby Cretaceous intrusions of the Tombstone suite are associated with intrusion-hosted and skarn W±Cu mineralization (Chakungal and Bennett, 2011). The Tiger Au deposit, in Silurian to Devonian carbonate rocks with basalt intercalations, lies west of the Nadaleen trend of Carlin-type occurrences and is probably related to the Paleocene Rackla granitic pluton (Thiessen et al., 2012).

3. Data sources and methods

3.1. Regional geochemical survey database

Since 1976, the joint federal National Geochemical Reconnaissance (NGR) and provincial Regional Geochemical Survey (RGS) programs have been carried out in British Columbia and Yukon to aid exploration and development of mineral resources. Sample collection, preparation, and analytical protocols are strictly specified and carefully monitored to ensure consistent data regardless of the area, year of survey, or analytical laboratory (Friske and Hornbrook,

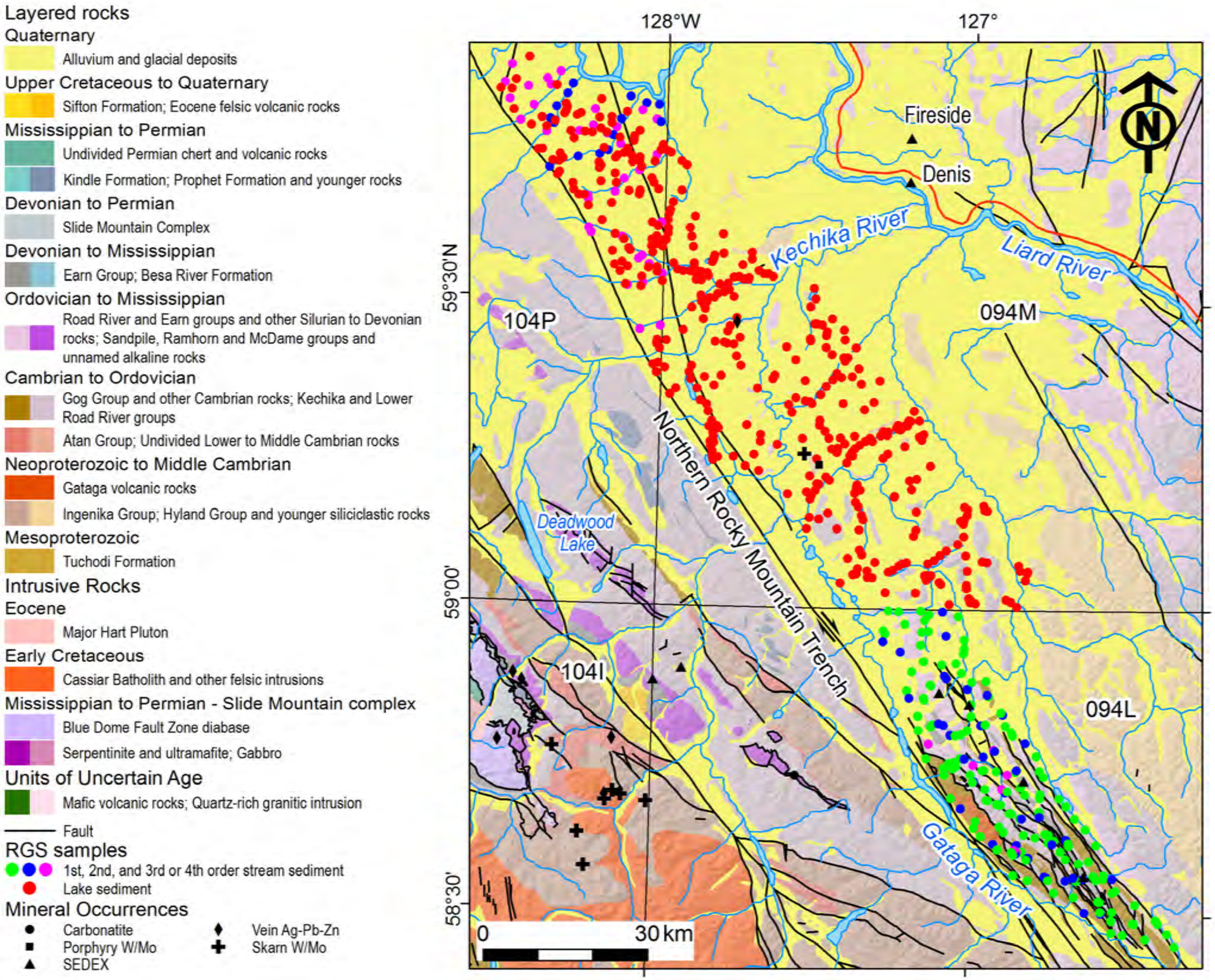

Fig. 2. Geology, selected Regional Geochemical Survey lake- and stream-sediment sample locations, and mineral occurrences, Kechika trough study area, north-central British Columbia. Geology after Gabrielse (1962; 1963a, b; 1998), and Ferri et al., (1999).

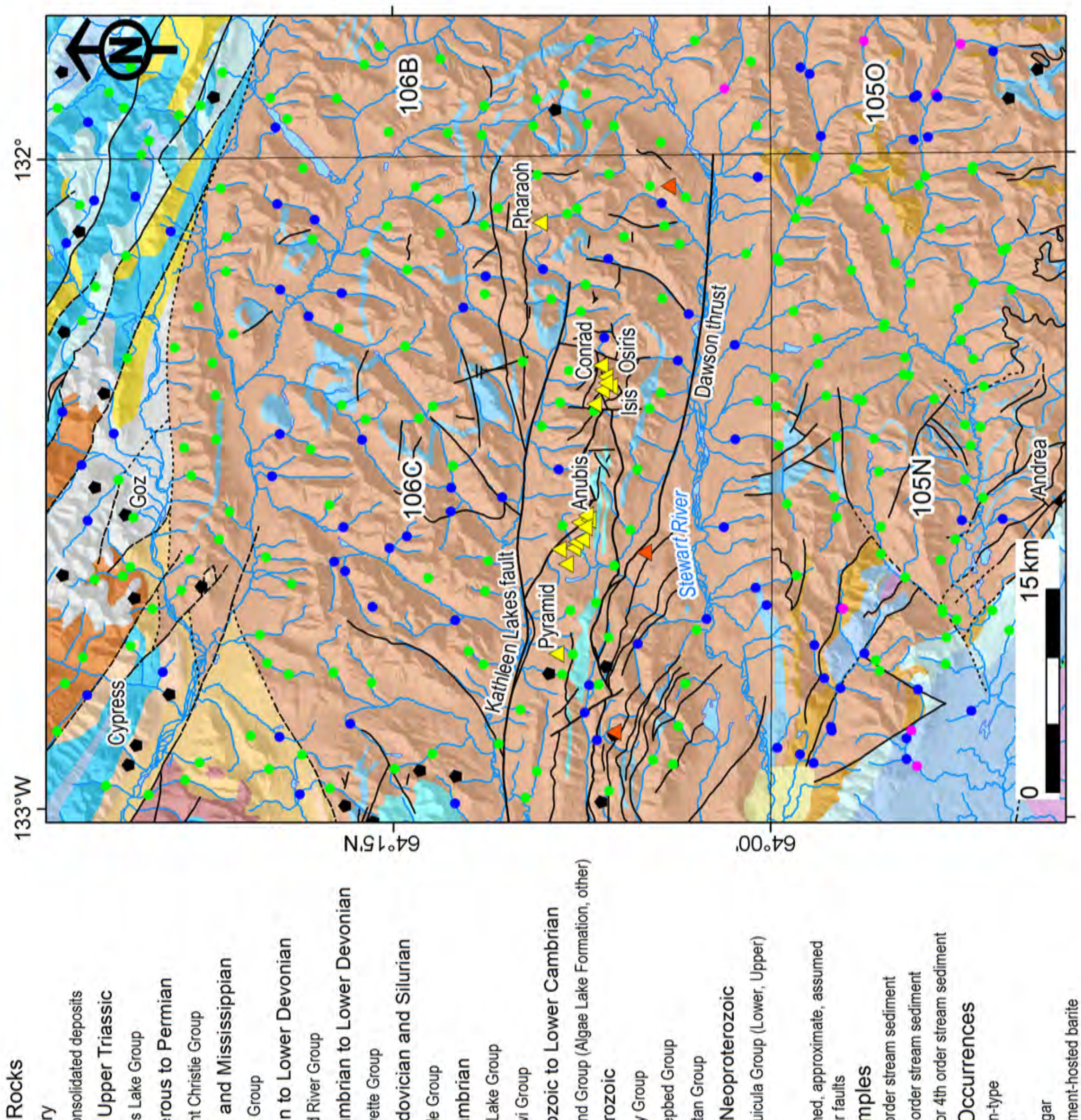

Fig. 3. Geology, selected National Geochemical Reconnaissance stream-sediment sample locations, and mineral occurrences, Rackla belt, east-central Yukon. Geology after Blusson (1974), Gordey and Makepeace, (1999), Chakungal and Bennett (2011), Colpron (2012), and Colpron et al. (2013).

1991).

The data for this study are derived from NGR and RGS stream- and lake-sediment geochemical surveys covering the Kechika trough of north-central British Columbia (total 644 samples) and the Rackla belt of Carlin-type occurrences in east-central Yukon (total 304 samples). To provide representative geochemical data for the catchment basin upstream, samples of fine-grained (<0.18 mm) sediment were collected from lakes at an average density of about 1 site per 11.2 km^2 and from streams at an average density of about 1 site per 7–13 km^2. These data include determinations for up to 63 analytes, field observations, and sample locations.

3.2. Raw data

We used multi-element determinations by aqua-regia extraction with inductively coupled plasma mass/emission spectrometry (ICP-MS/ES) finish, and instrumental neutron activation analysis (INAA). Analytical results below lower detection limits (DL) were set to half the minimum lower DL value and those above the upper DL were set to that DL value. The number of censored values less than the lower DL is generally <15% of the total number of determinations for most analytes, with the exception of Au by INAA, Co, Cs, Eu, Hf, Lu, Rb, Ta, Tb, Te, Ti and W for which 18–98% of the total number of values are ≤DL (Table 1).

Elsewhere (Rukhlov et al., 2014) we provide full appendices summarizing statistics for samples from the Kechika trough and the Rackla belt, grouped by sample medium, stream order, and bedrock geology. Univariate histograms, Tukey box plots and probability plots show typical positively skewed distributions of raw data for most analytes (Rukhlov et al., 2014). We used stream order as a rough approximation of catchment basin size to evaluate downstream dilution effects (Hawkes, 1976). The RGS sediments from third- and fourth-order streams have much lower concentrations of Al, Mg, P and most trace metals, and much higher Cr, Na, Ti and Ta concentrations than those from first-order streams due to the dilution by increased input of total sediment in the larger catchment basins (Rukhlov et al., 2014). Stream sediments derived primarily from thick, relatively far-travelled glacial and alluvial sediments in large catchment basins may miss the geochemical signal from material eroded from more immediate catchment basin slopes due to the decoupling effect (Fletcher, 1997; Heberlein, 2013).

Variable sample media and catchment basin geology may also influence sediment composition and cause background variations that can mask signals of mineralization (e.g., Bonham-Carter and Goodfellow, 1986). The RGS sediments show significant variations of Al, Bi, Ca, Ce, Hf, Pb, Rb, S, Sr and Th concentrations related to underlying geology. These elements, along with Br, Cr, Cs, rare-earth elements (REE) and Se, also have different concentrations in lake and stream sediments (Rukhlov et al., 2014).

3.3. Data standardization

To correct for the above effects, the raw analytical data were log10-transformed to a more normally distributed form, and levelled using the Z-score method, first by sample medium and stream order and then by underlying bedrock in ioGAS® software. Z-scores convert data to units of standard deviation using the median as a robust estimate of the mean and the interquartile range (IQR) multiplied by 0.7413 as a robust

Table 1. Summary of analytical detection levels (DL) for selected RGS data.

Analyte	Minimum DL	Values ≤DL (%)[1]
Ag	2 ppb	0.3
Al	0.01 wt %	0.9
As	0.1 ppm	5.6
Au	0.2 ppb	13.6
Au INAA	2 ppb	60.1
Ba INAA	50 ppm	0.5
Bi	0.02 ppm	11.1
Br INAA	0.5 ppm	3.5
Ca	0.01 wt %	0.3
Cd	0.01 ppm	0.3
Ce INAA	3/5 ppm	8.6
Co INAA	1/5 ppm	30.4
Cr INAA	5/20 ppm	7.1
Cs INAA	0.5/1 ppm	32.3
Cu	0.01 ppm	0.3
Eu INAA	0.2/1/2 ppm	46.6
Fe INAA	0.01 wt %	0
Ga	0.1 ppm	3.8
Hf INAA	1 ppm	22.9
Hg	5 ppb	2.1
K	0.01 wt %	8.3
La INAA	0.5/2 ppm	0.3
Lu INAA	0.05/0.2 ppm	19.6
Mg	0.01 wt %	0.3
Mn	1 ppm	0.3
Mo	0.01 ppm	0.3
Na INAA	0.01 wt %	0.2
Ni	0.1 ppm	0.5
P	0.001 wt %	0.3
Pb	0.01 ppm	0.3
Rb INAA	5/15 ppm	21.6
S	0.01/0.02 wt %	8.1
Sb	0.02 ppm	0.4
Sc INAA	0.1/0.2 ppm	0.7
Se	0.1 ppm	6.1
Sm INAA	0.1 ppm	4.8
Sr	0.5 ppm	0.3
Ta INAA	0.5 ppm	50.7
Tb INAA	0.5 ppm	50.9
Te	0.02 ppm	35.0
Th INAA	0.2 ppm	2.3
Ti	0.001 wt %	17.7
Tl	0.02 ppm	9.8
U INAA	0.5 ppm	0.4
V	2 ppm	6.3
W	0.1/0.2 ppm	98.1
Zn	0.1 ppm	0.3

Notes:
Determinations are by aqua regia extraction with inductively coupled plasma mass spectrometry or emission spectrometry finish and by instrumental neutron activation analysis (INAA) where indicated. [1]Per cent of total 948 values except for Au by inductively coupled plasma mass spectrometry (total 655 values).

estimate of standard deviation (SD). IQR is the difference between the 75th and 25th percentiles and covers approximately 50% of the data distribution (Garrett and Grunsky, 2001). After the transformation all levelled groups have a mean of zero and a SD of 1.The robust Z-score levelling preserves true outliers and is defined as follows:

Z = (Input Value – Median of group)/[Interquartile Range of group]*0.7413

Comparison of univariate raw and standardized data shows that the logarithmic transformation coupled with the robust Z-score levelling results in a de-skewed and statistically equivalent dataset (Rukhlov et al., 2014). All interpretations of the RGS data presented below are based on the standardized values.

4. Multi-element interpretation of Carlin-type signal

The standardized data were evaluated for Carlin-type geochemical signals using coincident As±Hg±Tl±Sb±Au anomalies, regression analysis, principal components analysis (PCA), and weighted sum (WS) index to test for geochemical patterns found in the Nevada type area (Patterson and Muntean, 2011). The model Carlin-type geochemical signatures in stream and lake sediments were validated by predicting the known Carlin-type occurrences of the Rackla belt.

4.1. Coincident pathfinder anomalies

Elevated concentrations of As±Hg±Tl±Sb±Au in regional stream and lake sediments that are underlain by favourable geology could signal Carlin-type mineralization (Tucker et al., 2013). In Figures 4 to 7, we illustrate sediment samples having As-Hg-Sb and As-Hg-Tl values greater than the 95 percentile and Au percentile ranks for the Kechika trough and the Rackla belt. Coincident As±Hg±Tl±Sb±Au anomalies highlight the main clusters of Carlin-type showings of the Rackla belt. Notably, Sb is less significant in samples nearest to the Carlin-type occurrences, similar to the geochemical signature of many Carlin deposits in Nevada (Patterson and Muntean, 2011).

Many stream and lake sediment samples in the Kechika trough also have As±Hg±Tl±Sb±Au concentrations greater than the 95 percentile. In the southeast part of the study area (NTS 094L) is a cluster of stream-sediment samples with elevated As±Au, Hg±Au, As-Hg, Hg-Tl, Sb-Tl, As-Tl-Sb, and As-Hg-Tl-Sb concentrations (Figs. 4 and 6). The only sample that shows coincident As-Hg-Tl-Sb anomalies is from a first-order catchment that is underlain by variably graphitic, calcareous, and pyritic, fine-grained siliciclastic and carbonate rocks, containing siliceous and baritic exhalites of the Earn Group. However, interpretation of these pathfinder signals may be obscured by nearby MVT, VMS, and SEDEX mineralization (Ferri et al., 1999; Chakungal and Bennett, 2011) at shelf–slope transitions.

4.2. Regression analysis

Late-stage realgar and orpiment are important spatial indicators of Carlin deposits in Nevada (Arehart, 1996) and the Rackla belt (Arehart et al., 2013; Tucker et al., 2013). As vs. S regression analysis on the RGS data provides an effective way to test for these indicators in the stream and lake sediments. Compared to a regular least-squares regression, a robust regression using the least median of squares (LMS) method of Rousseeuw and Leroy (1987) better models most of the data and enhances the identification of anomalies by down-weighting outlying data points. The method uses the following algorithm.

1. Randomly select many sub-groups, with the minimum size of each sub-group being equal to the number of response variables plus 1.
2. Calculate squared residuals (r^2) for all data using regression equations determined for each sub-group.
3. Calculate the residual (r_i) for each sample using the regression equation that gives the minimum median squared residual.
4. Estimate a preliminary standard deviation (s^0) of the minimum median squared residuals.
5. Assign a weight of 1 to samples having standardized residual, $r_i/s^0 < 3.0$, and a weight of 0 to the rest of samples.
6. Repeat a robust estimate of the standard deviation (s*) of the minimum median squared residuals on just the samples that had been assigned a weight of 1 in the previous step.
7. Assign a weight of 1 to samples having standardized residual, now calculated as $r_i/s^* < 3.0$, and a weight of 0 to the rest of samples.
8. Perform the least-squares regression on the samples having a weight of 1.
9. Calculate the final standardized residuals for all the data based on the regression solution in step 8.

Figure 8a shows the results of As vs. S regression analysis using the LMS method on the standardized RGS data. All but one of the stream and lake sediment samples with the standardized residuals of >3.0 fall along the realgar/orpiment control line on the As vs. S plot in terms of the raw concentrations (Fig. 8b). The only outlier is a lake sediment sample (Anomaly number 11; Rukhlov et al., 2014) containing 8.0 wt % S and 295 ppm As. These 'indicator mineral' standardized residuals mark two lake sediment and one stream sediment samples in the Kechika trough (Fig. 9), and highlight the main clusters of the Carlin-type occurrences and a number of new targets in the Rackla belt (Fig. 10).

4.3. Principal components analysis (PCA)

Robust PCA describes the variation within a multivariate dataset using a few derived functions, termed "principal components" (PC1, PC2, etc.), which are not biased by outliers (Campbell, 1980). The principal components are linear transformations of input variables representing perpendicular best-fit lines through the variation for all variables. The first few principal components account for most of the variance

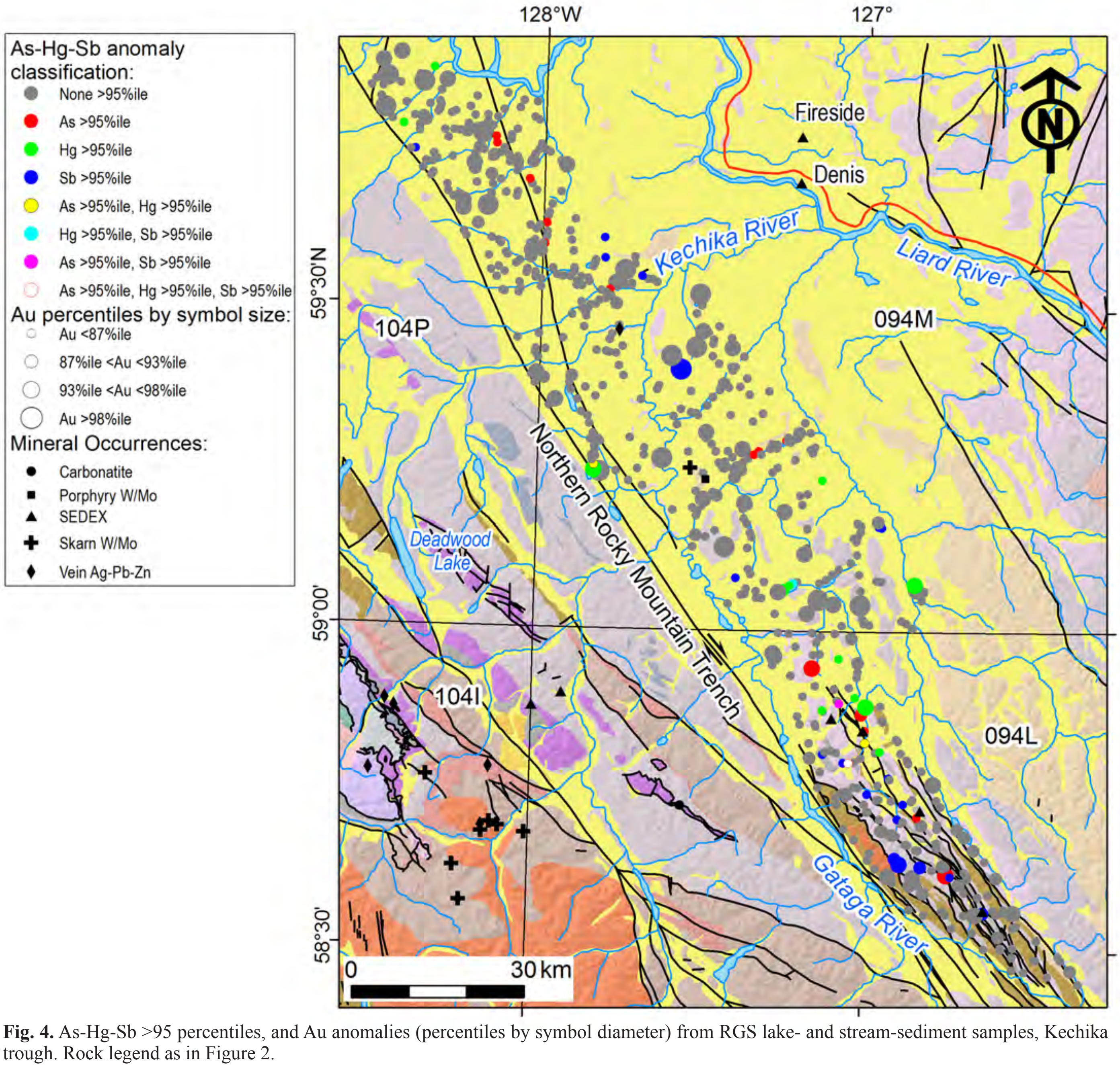

Fig. 4. As-Hg-Sb >95 percentiles, and Au anomalies (percentiles by symbol diameter) from RGS lake- and stream-sediment samples, Kechika trough. Rock legend as in Figure 2.

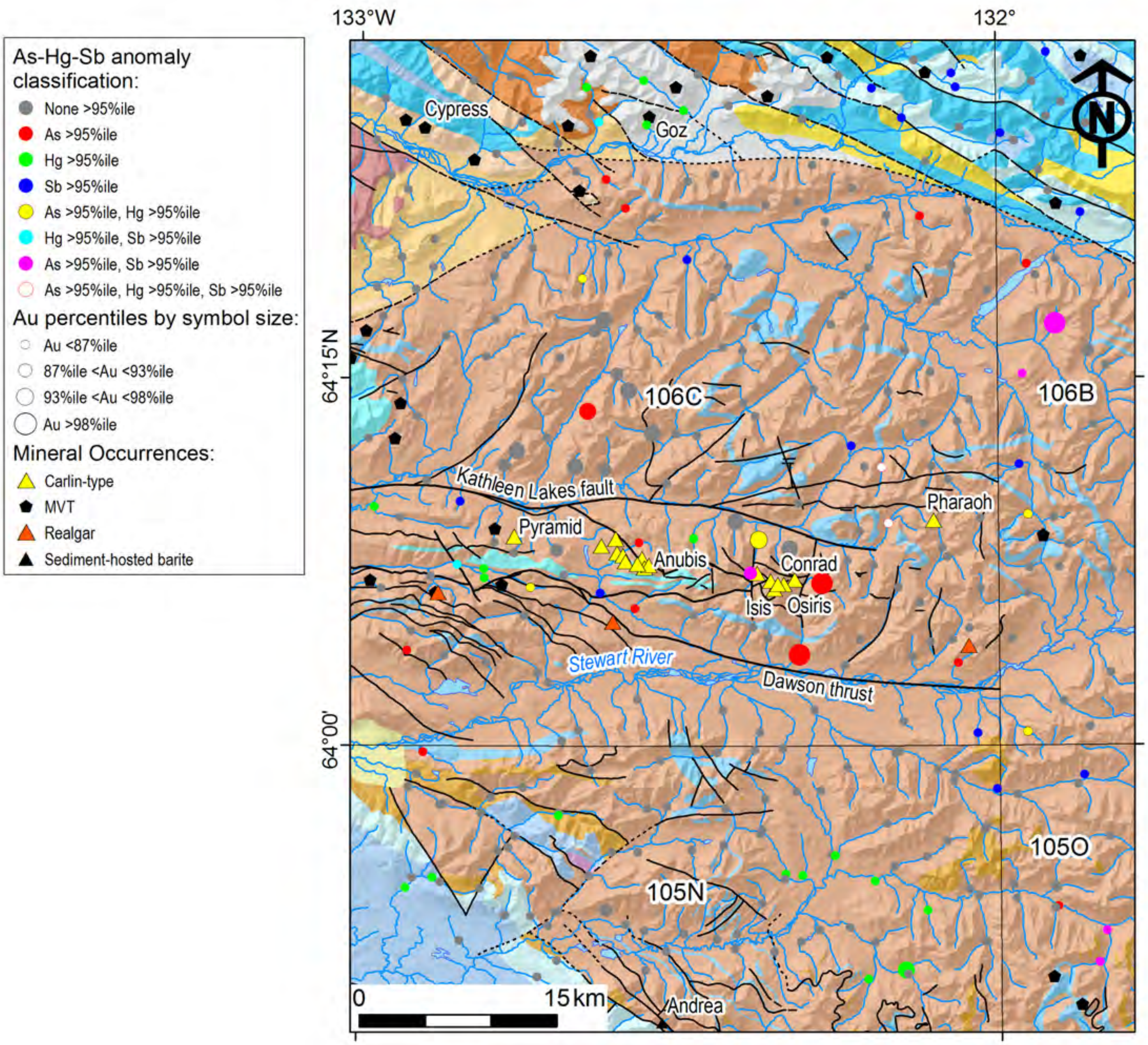

Fig. 5. As-Hg-Sb >95 percentiles, and Au anomalies (percentiles by symbol diameter) from NGR stream-sediment samples, Rackla belt. Rock legend as in Figure 3.

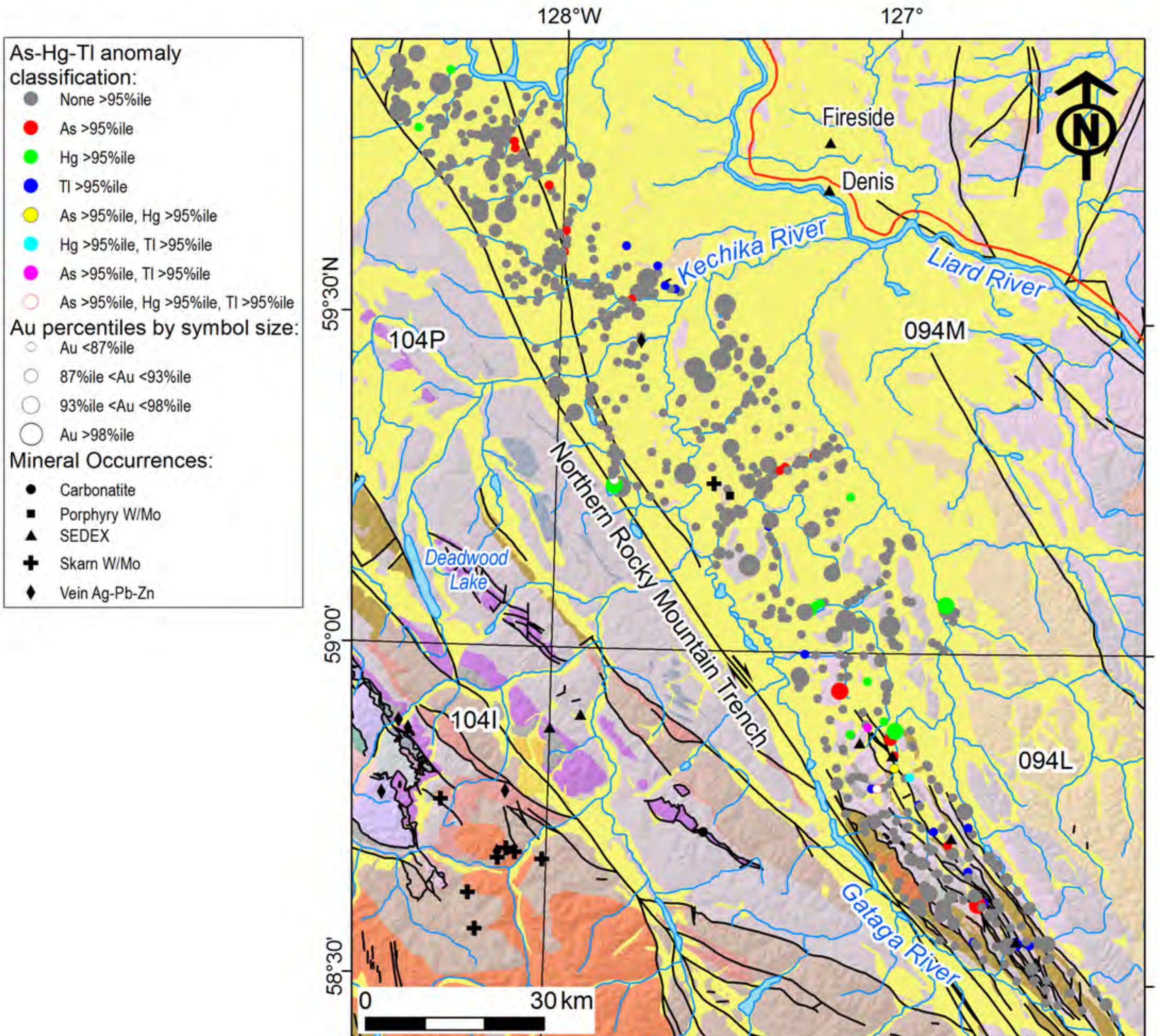

Fig. 6. As-Hg-Tl>95 percentiles, and Au anomalies (percentiles by symbol diameter) from RGS lake- and stream-sediment samples, Kechika trough. Rock legend as in Figure 2.

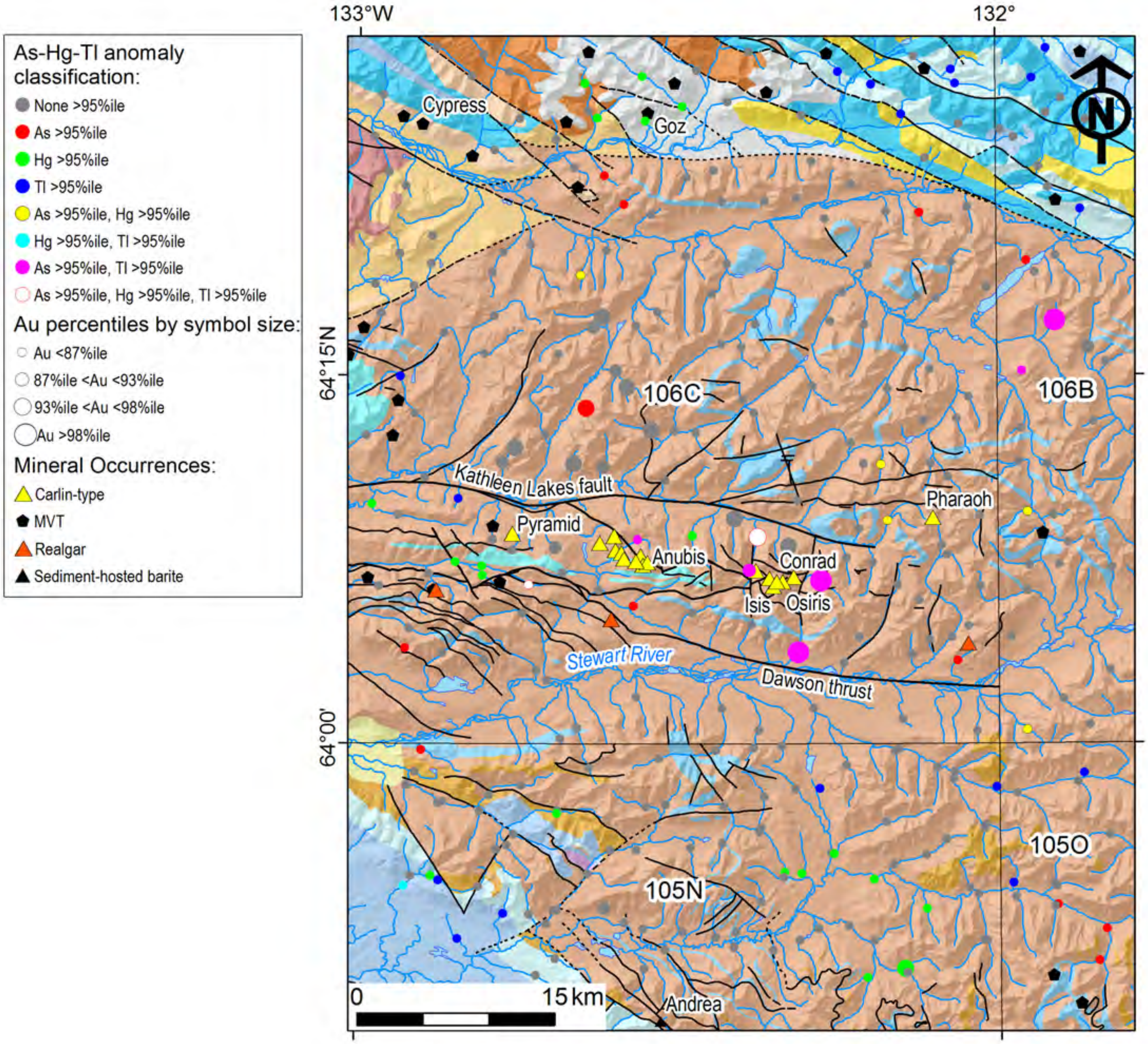

Fig. 7. As-Hg-Tl>95 percentiles, and Au anomalies (percentiles by symbol diameter) from NGR stream-sediment samples, Rackla belt. Rock legend as in Figure 3.

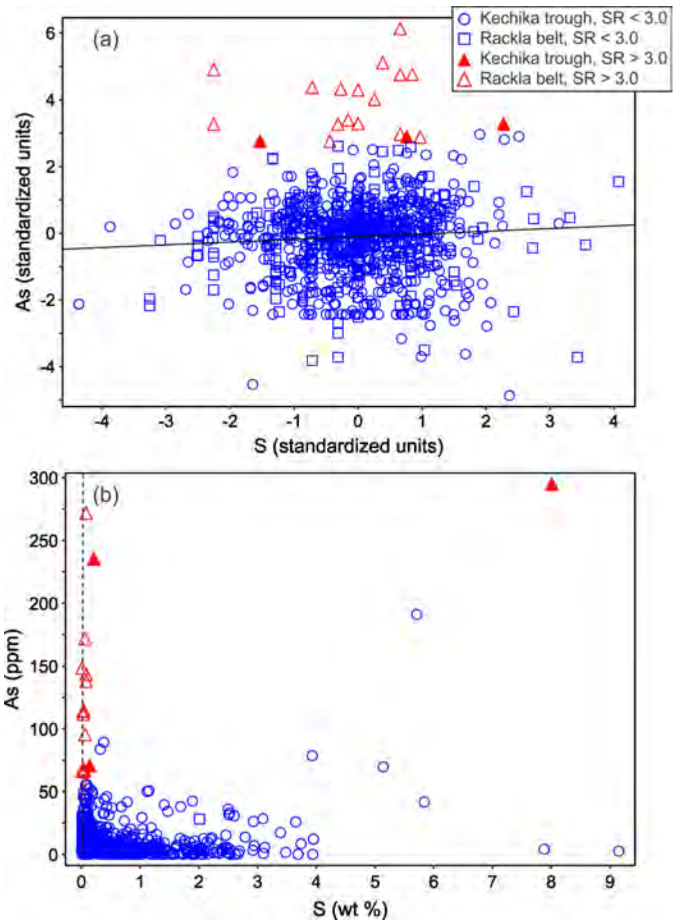

Fig. 8. As vs. S scatter plot for lake- and stream-sediment samples from the Kechika trough, and the Rackla belt. **a)** Standardized values showing the results of robust regression analysis. **b)** Raw concentrations indicating possible realgar control in the samples having standardized residuals (SR) >3.0.

and, therefore, capture the essential information in the original multi-dimensional dataset of the input variables (Rock, 1988).

We performed PCA on the standardized RGS data in ioGAS® software using a 46-element correlation matrix (Table 2). To minimize the impact of outliers on the principal components, the correlation matrix was calculated by weighting each of the samples by their robustly estimated Mahalanobis distance using a low outlier rejection algorithm. This method assigns low weights to outlying samples to minimize their influence on the correlation calculation, but then projects the outliers onto the robustly determined principal components (Campbell, 1980).

The robust PCA best discriminates the stream-sediment samples derived from Carlin-type showings of the Rackla belt in terms of the second (PC2) and the fourth (PC4) principal components, which total to ~16.6% of the variation in the original dataset (Table 3). On the PC4 vs. PC2 diagram (Fig. 11), data points that fall in the narrow field defined by this group of stream sediments have a similar multi-element, Carlin-type signature. They include one lake sediment sample, underlain by Cambrian–Ordovician carbonate and fine-grained siliciclastic strata of the Kechika Group in Kechika trough (Fig. 12), and a number of stream-sediment samples in the Rackla belt (Fig. 13).

A circle plot of scaled loadings of each variable to PC2 and PC4 shows a loose cluster of As, Hg, Tl, Te, Ba and Ag (Fig. 14). Sb plots away from this Carlin-type cluster. Similar geochemical signatures characterize many Carlin deposits in Nevada (e.g., Patterson and Muntean, 2011).

4.4. Weighted sum index (WS)

WS index uses a priori knowledge of mineralization to model its multi-element signature by a single linear function. The index is similar to the first principal component in PCA, but the relative weights for each element are assigned by the user, rather than being determined from the covariance or correlation matrix (Garrett and Grunsky, 2001).

Table 4 lists the model parameters for WS index of a Carlin-type signature in the RGS stream- and lake-sediment samples. Elements chosen for the WS index show the largest absolute loadings to a Carlin-type factor derived from the factor analysis on >6,400 drill-core samples from the Jerritt Canyon district in Nevada (Patterson and Muntean, 2011). Relative importance is assigned for each element based on their Carlin-type factor loadings. For instance, As, Hg, and Tl, which show the maximum loadings to the Carlin-type factor, are given 5 times more weight than Ag, Fe, and W, which are more characteristic of background (Table 4). Positive importance signifies elevated concentrations of pathfinder elements associated with the Carlin-type model and negative importance indicates diagnostic depletions. The relative importance values are converted into weights by dividing each importance by the square root of the sum of the squares of all of the importance values, so that the sums of the squares of the weights equal unity. The WS index score for each sample is then calculated as a sum of these weights multiplied by the normal scores for each corresponding element included in the index. The normal score for each element is obtained using robust estimates of the mean (median) and the SD (IQR*0.7413) and the Z-score levelling equation given above (Garrett and Grunsky, 2001).

In the Kechika trough study area, five stream-sediment and three lake-sediment samples show the Carlin-type WS index scores >98 percentile (Fig. 15). These samples are underlain by Paleozoic and older fine-grained siliciclastic and carbonate rocks of the Earn, Road River, Kechika, and Hyland groups. The stream sediments with the WS scores >98% percentile also predict the main clusters of the Carlin-type showings and highlight a few additional targets in the Rackla belt (Fig. 16).

4.5. Summary of multi-element modelling of Carlin-type signal in stream and lake sediments

The coincident elevated concentrations of pathfinder elements, standardized residuals >3.0 from robust As vs. S regression analysis, and principal components analysis and weighted sum index scores highlight a Carlin-type signal in 11

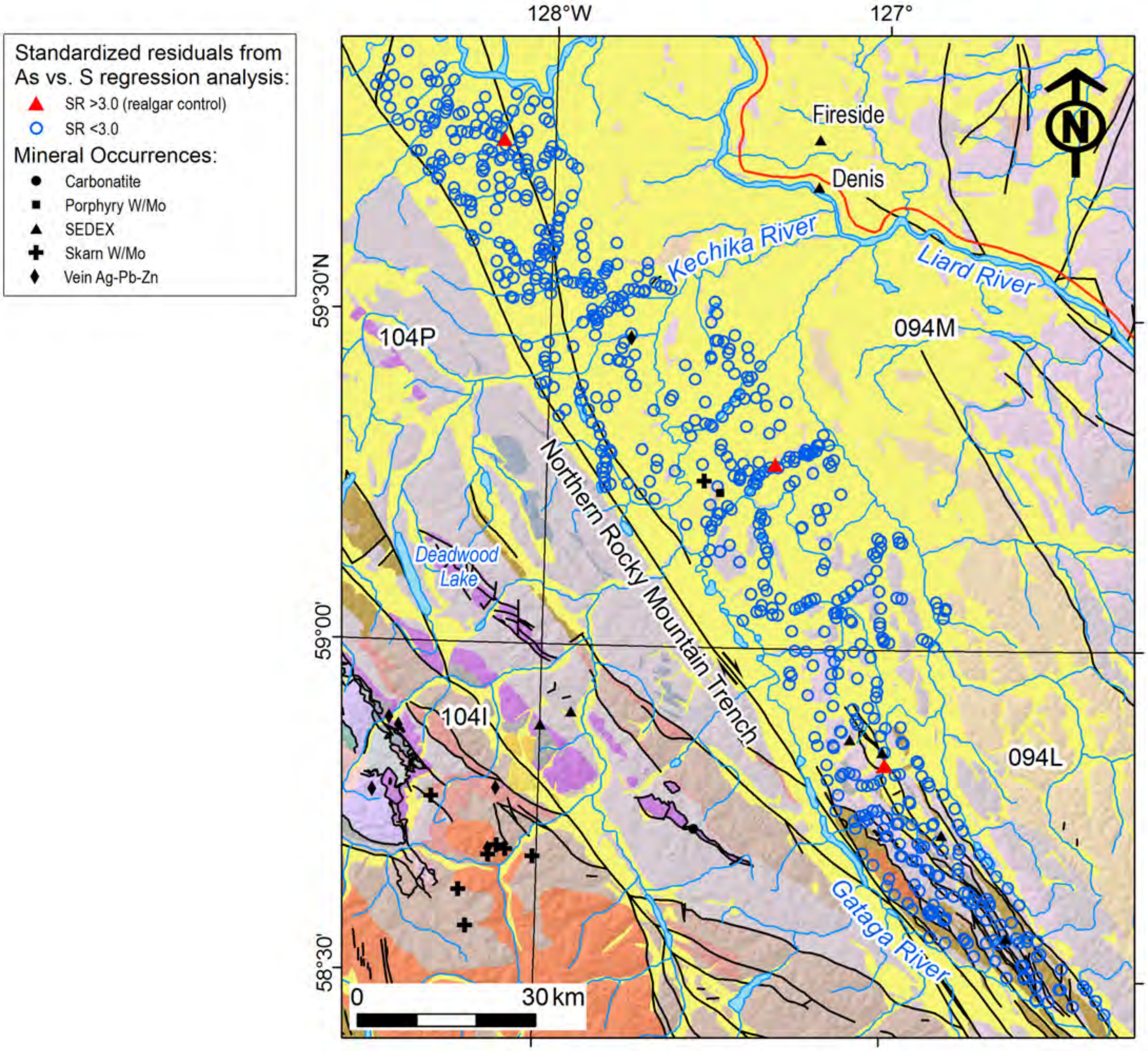

Fig. 9. As vs. S robust regression analysis on the RGS data, Kechika trough, highlighting standardized residuals (SR) >3.0, which may indicate realgar. Rock legend as in Figure 2.

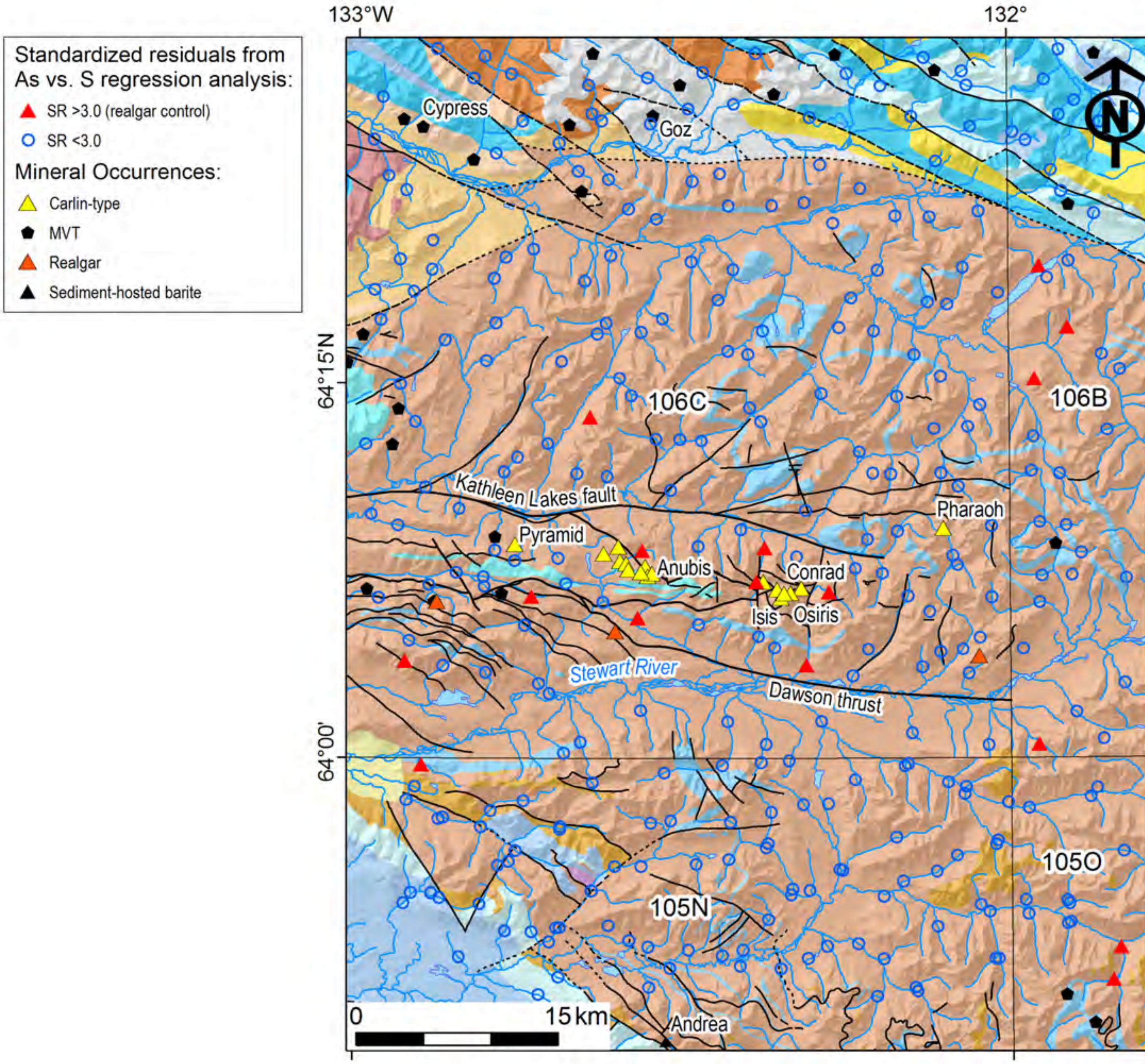

Fig. 10. As vs. S robust regression analysis on the NGR data, Rackla belt, highlighting standardized residuals (SR) >3.0, which may indicate realgar. Rock legend as in Figure 3.

Table 2. Correlation matrix for input variables used in PCA on the RGS/NGR lake- and stream-sediment samples.

	Eu	Tb	W	Au	Ag	Al	As	Bi	Br	Ca	Cd	Ce	Co	Cr	Ba	Cs	Cu	Fe	Ga	Hf	Hg	K	La	Lu	Mg	Mn	Mo	Na	Ni	P	Pb	Rb	S	Sb	Sc	Se	Sm	Sr	Ta	Te	Th	Ti	Tl	U	V	Zn
Eu		0.3	0.0	-0.1	-0.1	-0.1	0.0	-0.1	-0.1	-0.2	-0.2	0.0	-0.1	0.0	-0.1	-0.1	-0.1	0.0	-0.1	0.0	-0.1	-0.2	0.0	-0.1	-0.2	-0.1	-0.1	0.0	-0.1	-0.1	-0.2	-0.1	-0.2	-0.2	0.0	-0.2	0.0	-0.2	-0.1	-0.1	0.0	-0.2	-0.2	0.0	-0.2	-0.1
Tb	0.3		0.0	0.0	0.2	0.1	0.1	0.2	-0.2	-0.1	0.1	0.2	0.2	0.2	0.2	0.1	0.2	0.1	0.1	0.3	0.1	0.0	0.2	0.2	0.0	0.0	-0.1	0.1	0.1	0.1	0.1	0.2	-0.2	0.0	0.1	-0.1	0.2	-0.1	0.1	0.1	0.2	0.0	0.1	0.0	0.1	0.1
W	0.0	0.0		0.0	0.1	0.1	-0.1	0.2	0.1	0.1	0.1	0.1	0.1	0.1	0.0	0.1	0.1	0.1	0.1	0.0	0.0	0.1	0.1	0.1	0.2	0.0	0.1	0.2	0.1	0.1	0.1	0.1	0.1	0.2	0.1	0.1	0.1	0.1	0.0	0.0	0.1	0.1	0.0	0.1	0.1	0.1
Au	-0.1	0.0	0.0		0.2	0.1	0.1	-0.1	0.0	-0.2	0.3	0.1	0.0	0.1	0.1	0.0	0.2	0.0	0.1	0.2	0.2	0.1	0.1	0.1	-0.1	0.0	0.1	0.1	0.2	0.2	0.0	0.0	0.0	0.3	0.1	0.1	0.1	-0.2	0.1	0.1	0.0	0.2	0.1	0.0	0.2	0.3
Ag	-0.1	0.2	0.1	0.2		0.4	0.2	0.4	0.1	-0.3	0.7	0.4	0.3	0.6	0.4	0.4	0.7	0.3	0.3	0.4	0.6	0.4	0.4	0.5	0.0	-0.1	0.3	0.1	0.7	0.7	0.5	0.4	-0.1	0.5	0.5	0.3	0.5	-0.3	0.3	0.2	0.4	0.0	0.6	0.0	0.6	0.7
Al	-0.1	0.1	0.1	0.1	0.4		0.1	0.7	-0.3	-0.5	0.3	0.8	0.7	0.7	0.4	0.6	0.6	0.5	1.0	0.6	0.3	0.7	0.8	0.7	0.2	0.1	-0.1	0.6	0.6	0.3	0.7	0.7	-0.3	0.1	0.8	-0.1	0.8	-0.5	0.4	0.0	0.8	0.0	0.4	-0.2	0.7	0.4
As	0.0	0.1	-0.1	0.1	0.2	0.1		0.3	-0.3	0.1	0.1	0.3	0.3	0.4	0.4	0.4	0.3	0.5	0.1	0.2	0.4	0.3	0.3	0.3	0.2	0.4	0.1	0.0	0.4	0.1	0.3	0.3	-0.1	0.3	0.3	-0.1	0.3	0.0	0.2	0.3	0.3	-0.1	0.4	-0.1	0.4	0.2
Bi	-0.1	0.2	0.2	-0.1	0.4	0.7	0.3		-0.3	-0.4	0.1	0.7	0.8	0.6	0.3	0.6	0.6	0.6	0.6	0.5	0.2	0.6	0.7	0.7	0.2	0.2	-0.1	0.3	0.5	0.2	0.9	0.8	-0.2	0.2	0.8	-0.2	0.7	-0.4	0.5	0.0	0.8	-0.3	0.3	-0.2	0.3	0.3
Br	-0.1	-0.2	0.1	0.0	0.1	-0.3	-0.3	-0.3		-0.1	0.1	-0.4	-0.3	-0.2	-0.4	-0.4	-0.1	-0.2	-0.3	-0.4	0.0	-0.3	-0.4	-0.2	-0.4	-0.1	0.3	-0.1	-0.2	0.4	-0.3	-0.5	0.3	0.2	-0.3	0.4	-0.3	0.0	-0.3	-0.2	-0.4	0.2	-0.2	0.3	-0.2	0.0
Ca	-0.2	-0.1	0.1	-0.2	-0.3	-0.5	0.1	-0.4	-0.1		-0.2	-0.3	-0.3	-0.3	0.0	-0.1	-0.5	0.0	-0.5	-0.4	-0.1	-0.3	-0.3	-0.4	0.5	0.2	0.1	-0.4	-0.3	-0.3	-0.3	-0.2	0.4	0.0	-0.4	0.2	-0.4	0.9	-0.2	0.3	-0.3	-0.1	-0.1	0.3	-0.2	-0.3
Cd	-0.2	0.1	0.1	0.3	0.7	0.3	0.1	0.1	0.1	-0.2		0.2	0.2	0.4	0.4	0.2	0.6	0.1	0.3	0.3	0.6	0.3	0.2	0.3	-0.1	-0.1	0.4	0.1	0.6	0.5	0.2	0.2	0.1	0.7	0.3	0.5	0.2	-0.3	0.2	0.1	0.2	0.2	0.6	0.0	0.6	0.9
Ce	0.0	0.2	0.1	0.1	0.4	0.8	0.3	0.7	-0.4	-0.3	0.2		0.8	0.8	0.5	0.7	0.6	0.6	0.8	0.8	0.4	0.6	1.0	0.9	0.3	0.1	-0.2	0.5	0.6	0.2	0.8	0.9	-0.3	0.1	0.9	-0.1	1.0	-0.4	0.5	0.0	0.9	-0.2	0.5	-0.2	0.6	0.4
Co	-0.1	0.2	0.1	0.0	0.3	0.7	0.3	0.8	-0.3	-0.3	0.2	0.8		0.6	0.4	0.7	0.6	0.6	0.6	0.6	0.3	0.6	0.7	0.7	0.3	0.3	-0.1	0.3	0.6	0.1	0.8	0.8	-0.2	0.2	0.8	-0.1	0.7	-0.4	0.4	0.1	0.8	-0.2	0.5	-0.1	0.5	0.3
Cr	0.0	0.2	0.1	0.1	0.6	0.7	0.4	0.6	-0.2	-0.3	0.4	0.8	0.6		0.6	0.6	0.7	0.6	0.6	0.6	0.5	0.6	0.8	0.8	0.3	0.0	0.0	0.5	0.7	0.4	0.7	0.7	-0.3	0.3	0.9	0.1	0.8	-0.4	0.4	0.1	0.8	-0.1	0.6	-0.1	0.7	0.5
Ba	-0.1	0.2	0.0	0.1	0.4	0.4	0.4	0.3	-0.4	0.0	0.4	0.5	0.4	0.6		0.4	0.5	0.5	0.4	0.4	0.5	0.5	0.5	0.4	0.3	0.2	0.1	0.2	0.5	0.3	0.3	0.5	-0.2	0.3	0.5	0.2	0.4	-0.1	0.3	0.1	0.5	0.0	0.6	0.0	0.6	0.4
Cs	-0.1	0.1	0.1	0.0	0.4	0.6	0.4	0.6	-0.4	-0.1	0.2	0.7	0.7	0.6	0.4		0.5	0.5	0.5	0.5	0.4	0.6	0.7	0.6	0.4	0.1	0.0	0.2	0.6	0.1	0.7	0.8	-0.2	0.2	0.7	-0.1	0.7	-0.2	0.4	0.2	0.8	-0.2	0.5	-0.1	0.5	0.3
Cu	-0.1	0.2	0.1	0.2	0.7	0.6	0.3	0.6	-0.1	-0.5	0.6	0.6	0.6	0.7	0.5	0.5		0.5	0.6	0.4	0.6	0.6	0.6	0.6	0.0	0.1	0.3	0.2	0.8	0.5	0.6	0.6	-0.1	0.6	0.7	0.2	0.6	-0.5	0.3	0.2	0.6	0.0	0.6	0.0	0.7	0.7
Fe	0.0	0.1	0.1	0.0	0.3	0.5	0.5	0.6	-0.2	0.0	0.1	0.6	0.6	0.6	0.5	0.5	0.5		0.4	0.3	0.4	0.4	0.6	0.6	0.3	0.5	0.1	0.2	0.5	0.2	0.5	0.6	0.0	0.2	0.6	0.1	0.6	-0.1	0.3	0.1	0.5	-0.1	0.4	0.0	0.5	0.3
Ga	-0.1	0.1	0.1	0.1	0.3	1.0	0.1	0.6	-0.3	-0.5	0.3	0.8	0.6	0.6	0.4	0.5	0.6	0.4		0.6	0.2	0.7	0.8	0.7	0.2	0.1	-0.1	0.6	0.5	0.2	0.6	0.7	-0.3	0.1	0.8	-0.1	0.7	-0.5	0.4	0.0	0.8	0.1	0.4	-0.2	0.7	0.3
Hf	0.0	0.3	0.0	0.2	0.4	0.6	0.2	0.5	-0.4	-0.4	0.3	0.8	0.6	0.6	0.4	0.5	0.4	0.3	0.6		0.3	0.4	0.8	0.8	0.1	-0.1	-0.3	0.5	0.5	0.2	0.6	0.7	-0.4	0.1	0.7	-0.1	0.8	-0.4	0.4	-0.1	0.8	-0.1	0.3	-0.2	0.4	0.3
Hg	-0.1	0.1	0.0	0.2	0.6	0.3	0.4	0.2	0.0	-0.1	0.6	0.4	0.3	0.5	0.5	0.4	0.6	0.4	0.2	0.3		0.5	0.4	0.4	0.1	0.1	0.3	0.0	0.7	0.4	0.4	0.4	0.0	0.6	0.5	0.3	0.4	-0.2	0.3	0.2	0.4	0.0	0.7	-0.1	0.6	0.7
K	-0.2	0.0	0.1	0.1	0.4	0.7	0.3	0.6	-0.3	-0.3	0.3	0.6	0.6	0.6	0.5	0.6	0.6	0.4	0.7	0.4	0.5		0.6	0.5	0.4	0.2	0.1	0.2	0.6	0.1	0.6	0.7	0.0	0.2	0.7	0.1	0.5	-0.3	0.3	0.3	0.6	0.0	0.7	0.0	0.7	0.4
La	0.0	0.2	0.1	0.1	0.4	0.8	0.3	0.7	-0.4	-0.3	0.2	1.0	0.7	0.8	0.5	0.7	0.6	0.6	0.8	0.8	0.4	0.6		0.9	0.4	0.1	-0.2	0.5	0.7	0.2	0.8	0.9	-0.3	0.2	0.9	-0.1	0.9	-0.4	0.4	0.1	1.0	-0.2	0.5	-0.1	0.6	0.4
Lu	-0.1	0.2	0.1	0.1	0.5	0.7	0.3	0.7	-0.2	-0.4	0.3	0.9	0.7	0.8	0.4	0.6	0.6	0.6	0.7	0.8	0.4	0.5	0.9		0.2	0.0	-0.1	0.4	0.7	0.3	0.8	0.8	-0.3	0.3	0.9	0.0	0.9	-0.4	0.4	0.0	0.9	-0.1	0.5	-0.1	0.5	0.4
Mg	-0.2	0.0	0.2	-0.1	0.0	0.2	0.2	0.2	-0.4	0.5	-0.1	0.3	0.3	0.3	0.3	0.4	0.0	0.3	0.2	0.1	0.1	0.4	0.4	0.2		0.2	0.0	0.1	0.2	-0.1	0.3	0.4	0.1	0.2	0.3	0.0	0.3	0.5	0.2	0.4	0.3	-0.1	0.3	0.2	0.3	0.0
Mn	-0.1	0.0	0.0	0.0	-0.1	0.1	0.4	0.2	-0.1	0.2	-0.1	0.1	0.3	0.0	0.2	0.1	0.1	0.5	0.1	-0.1	0.1	0.2	0.1	0.0	0.2		0.1	-0.1	0.2	0.0	0.1	0.1	0.1	0.1	0.1	0.0	0.0	0.1	0.1	0.2	0.1	0.1	0.2	0.1	0.2	0.0
Mo	-0.1	-0.1	0.1	0.1	0.3	-0.1	0.1	-0.1	0.3	0.1	0.4	-0.2	-0.1	0.0	0.1	0.0	0.3	0.1	-0.1	-0.3	0.3	0.1	-0.2	-0.1	0.0	0.1		-0.2	0.3	0.2	-0.1	-0.1	0.4	0.6	-0.1	0.5	-0.2	0.2	-0.1	0.3	-0.2	0.1	0.3	0.5	0.3	0.4
Na	0.0	0.1	0.2	0.1	0.1	0.6	0.0	0.3	-0.1	-0.4	0.1	0.5	0.3	0.5	0.2	0.2	0.2	0.2	0.6	0.5	0.0	0.2	0.5	0.4	0.1	-0.1	-0.2		0.3	0.2	0.2	0.3	-0.3	-0.1	0.5	-0.2	0.5	-0.3	0.2	-0.2	0.4	0.3	0.1	-0.1	0.3	0.1
Ni	-0.1	0.1	0.1	0.2	0.7	0.6	0.4	0.5	-0.2	-0.3	0.6	0.6	0.6	0.7	0.5	0.6	0.8	0.5	0.5	0.5	0.7	0.6	0.7	0.7	0.2	0.2	0.3	0.3		0.4	0.6	0.6	0.0	0.7	0.7	0.2	0.6	-0.3	0.3	0.2	0.6	0.0	0.8	0.1	0.7	0.8
P	-0.1	0.1	0.1	0.2	0.7	0.3	0.1	0.2	0.4	-0.3	0.5	0.2	0.1	0.4	0.3	0.1	0.5	0.2	0.2	0.2	0.4	0.1	0.2	0.3	-0.1	0.0	0.2	0.2	0.4		0.2	0.1	-0.2	0.4	0.3	0.2	0.3	-0.3	0.0	0.0	0.2	0.2	0.3	-0.1	0.4	0.5
Pb	-0.2	0.1	0.1	0.0	0.5	0.7	0.3	0.9	-0.3	-0.3	0.2	0.8	0.8	0.7	0.3	0.7	0.6	0.5	0.6	0.6	0.4	0.6	0.8	0.8	0.3	0.1	-0.1	0.2	0.6	0.2		0.8	-0.2	0.2	0.8	-0.1	0.8	-0.4	0.4	0.1	0.9	-0.2	0.5	-0.1	0.5	0.4
Rb	-0.1	0.2	0.1	0.0	0.4	0.7	0.3	0.8	-0.5	-0.2	0.2	0.9	0.8	0.7	0.5	0.8	0.6	0.6	0.7	0.7	0.4	0.7	0.9	0.8	0.4	0.1	-0.1	0.3	0.6	0.1	0.8		-0.2	0.2	0.8	-0.1	0.8	-0.3	0.4	0.2	0.9	-0.2	0.5	-0.1	0.5	0.3
S	-0.2	-0.2	0.1	0.0	-0.1	-0.3	-0.1	-0.2	0.3	0.4	0.1	-0.3	-0.2	-0.3	-0.2	-0.2	-0.1	0.0	-0.3	-0.4	0.0	0.0	-0.3	-0.3	0.1	0.1	0.4	-0.3	0.0	-0.2	-0.2	-0.2		0.3	-0.3	0.5	-0.3	0.5	-0.2	0.1	-0.3	0.1	0.1	0.5	-0.1	0.1
Sb	-0.2	0.0	0.2	0.3	0.5	0.1	0.3	0.2	0.2	0.0	0.7	0.1	0.2	0.3	0.3	0.2	0.6	0.2	0.1	0.1	0.6	0.2	0.2	0.3	0.2	0.1	0.6	-0.1	0.7	0.4	0.2	0.2	0.3		0.2	0.4	0.2	0.0	0.1	0.2	0.1	0.1	0.5	0.3	0.5	0.7
Sc	0.0	0.1	0.1	0.1	0.5	0.8	0.3	0.8	-0.3	-0.4	0.3	0.9	0.8	0.9	0.5	0.7	0.7	0.6	0.8	0.7	0.5	0.7	0.9	0.9	0.3	0.1	-0.1	0.5	0.7	0.3	0.8	0.8	-0.3	0.2		0.0	0.9	-0.5	0.4	0.0	0.9	-0.1	0.6	-0.2	0.6	0.4
Se	-0.2	-0.1	0.1	0.1	0.3	-0.1	-0.1	-0.2	0.4	0.2	0.5	-0.1	-0.1	0.1	0.2	-0.1	0.2	0.1	-0.1	-0.1	0.3	0.1	-0.1	0.0	0.0	0.0	0.5	-0.2	0.2	0.2	-0.1	-0.1	0.5	0.4	0.0		-0.1	0.2	-0.1	0.1	-0.2	0.1	0.3	0.4	0.2	0.3
Sm	0.0	0.2	0.1	0.1	0.5	0.8	0.3	0.7	-0.3	-0.4	0.2	1.0	0.7	0.8	0.4	0.7	0.6	0.6	0.7	0.8	0.4	0.5	0.9	0.9	0.3	0.0	-0.2	0.5	0.6	0.3	0.8	0.8	-0.3	0.2	0.9	-0.1		-0.5	0.4	0.0	0.9	-0.2	0.4	-0.2	0.5	0.3
Sr	-0.2	-0.1	0.1	-0.2	-0.3	-0.5	0.0	-0.4	0.0	0.9	-0.3	-0.4	-0.4	-0.4	-0.1	-0.2	-0.5	-0.1	-0.5	-0.4	-0.2	-0.3	-0.4	-0.4	0.5	0.1	0.2	-0.3	-0.3	-0.3	-0.4	-0.3	0.5	0.0	-0.5	0.2	-0.5		-0.2	0.4	-0.4	0.0	-0.2	0.4	-0.3	-0.3
Ta	-0.1	0.1	0.0	0.1	0.3	0.4	0.2	0.5	-0.3	-0.2	0.2	0.5	0.4	0.4	0.3	0.4	0.3	0.3	0.4	0.4	0.3	0.3	0.4	0.4	0.2	0.1	-0.1	0.2	0.3	0.0	0.4	0.4	-0.2	0.1	0.4	-0.1	0.4	-0.2		0.0	0.5	-0.1	0.3	-0.1	0.3	0.2
Te	-0.1	0.1	0.0	0.1	0.2	0.0	0.3	0.0	-0.2	0.3	0.1	0.0	0.1	0.1	0.1	0.2	0.2	0.1	0.0	-0.1	0.2	0.3	0.1	0.0	0.4	0.2	0.3	-0.2	0.2	0.0	0.1	0.2	0.1	0.2	0.0	0.1	0.0	0.4	0.0		0.0	-0.1	0.3	0.2	0.2	0.1
Th	0.0	0.2	0.1	0.0	0.4	0.8	0.3	0.8	-0.4	-0.3	0.2	0.9	0.8	0.8	0.5	0.8	0.6	0.5	0.8	0.8	0.4	0.6	1.0	0.9	0.3	0.1	-0.2	0.4	0.6	0.2	0.9	0.9	-0.3	0.1	0.9	-0.2	0.9	-0.4	0.5	0.0		-0.2	0.5	-0.2	0.5	0.3
Ti	-0.2	0.0	0.1	0.2	0.0	0.0	-0.1	-0.3	0.2	-0.1	0.2	-0.2	-0.2	-0.1	0.0	-0.2	0.0	-0.1	0.1	-0.1	0.0	0.0	-0.2	-0.1	-0.1	0.1	0.1	0.3	0.0	0.2	-0.2	-0.2	0.1	0.1	-0.1	0.1	-0.2	0.0	-0.1	-0.1	-0.2		0.1	0.1	0.2	0.1
Tl	-0.2	0.1	0.0	0.1	0.6	0.4	0.4	0.3	-0.2	-0.1	0.6	0.5	0.5	0.6	0.6	0.5	0.6	0.4	0.4	0.3	0.7	0.7	0.5	0.5	0.3	0.2	0.3	0.1	0.8	0.3	0.5	0.5	0.1	0.5	0.6	0.3	0.4	-0.2	0.3	0.3	0.5	0.1		0.0	0.8	0.7
U	0.0	0.0	0.1	0.0	0.0	-0.2	-0.1	-0.2	0.3	0.3	0.0	-0.2	-0.1	-0.1	0.0	-0.1	0.0	0.0	-0.2	-0.2	-0.1	0.0	-0.1	-0.1	0.2	0.1	0.5	-0.1	0.1	-0.1	-0.1	-0.1	0.5	0.3	-0.2	0.4	-0.2	0.4	-0.1	0.2	-0.2	0.1	0.0		0.0	0.1
V	-0.2	0.1	0.1	0.2	0.6	0.7	0.4	0.3	-0.2	-0.2	0.6	0.6	0.5	0.7	0.6	0.5	0.7	0.5	0.7	0.4	0.6	0.7	0.6	0.5	0.3	0.2	0.3	0.3	0.7	0.4	0.5	0.5	-0.1	0.5	0.6	0.2	0.5	-0.3	0.3	0.2	0.5	0.2	0.8	0.0		0.7
Zn	-0.1	0.1	0.1	0.3	0.7	0.4	0.2	0.3	0.0	-0.3	0.9	0.4	0.3	0.5	0.4	0.3	0.7	0.3	0.3	0.3	0.7	0.4	0.4	0.4	0.0	0.0	0.4	0.1	0.8	0.5	0.4	0.3	0.1	0.7	0.4	0.3	0.3	-0.3	0.2	0.1	0.3	0.1	0.7	0.1	0.7	

Notes:

Correlation matrix was calculated using log10-transformed and levelled values by weighting each of the samples by their robustly estimated Mahalanobis distance to minimize the impact of outliers on the principal components. The Mahalanobis distance (D_M) is the distance of a multivariate observation to a centroid or multivariate mean of a group of observations and is defined as follows: $D_M^2 = [x - \mu]' C^{-1}[x - \mu]$ where x is a vector of an observation, μ is the mean, and C is the covariance matrix (Grunsky, 2007).

Table 3. Results of robust PCA for the second and fourth principal components that best discriminate stream sediments associated with Carlin-type occurrences of the Rackla belt, east-central Yukon.

Principal Component	PC2		PC4	
	Eigenvectors[1]	Scaled coordinates[4]	Eigenvectors[1]	Scaled coordinates[4]
Au	0.11	0.27	-0.01	-0.01
Ag	0.19	0.46	0.12	0.18
Al	-0.09	-0.21	-0.20	-0.28
As	0.07	0.16	0.31	0.43
Bi	-0.12	-0.28	-0.02	-0.03
Br INAA	0.15	0.36	-0.19	-0.27
Ca	0.09	0.22	-0.03	-0.05
Cd	0.28	0.67	0.04	0.06
Ce INAA	-0.12	-0.28	-0.04	-0.05
Co INAA	-0.07	-0.16	-0.03	-0.05
Cr INAA	0.00	0.01	0.01	0.02
Ba INAA	0.09	0.22	0.13	0.19
Cs INAA	-0.04	-0.10	0.05	0.07
Cu	0.14	0.32	0.05	0.07
Eu INAA	-0.12	-0.29	0.26	0.36
Fe INAA	0.02	0.04	0.03	0.04
Ga	-0.09	-0.21	-0.25	-0.35
Hf INAA	-0.12	-0.29	-0.01	-0.01
Hg	0.21	0.51	0.22	0.31
K	0.05	0.11	-0.09	-0.12
La INAA	-0.10	-0.25	-0.05	-0.08
Lu INAA	-0.06	-0.15	-0.02	-0.02
Mg	0.02	0.04	-0.16	-0.23
Mn	0.05	0.12	0.04	0.06
Mo	0.32	0.76	-0.03	-0.05
Na INAA	-0.13	-0.31	-0.35	-0.50
Ni	0.16	0.39	0.05	0.06
P	0.15	0.34	0.00	0.00
Pb	-0.07	-0.16	-0.02	-0.03
Rb INAA	-0.08	-0.20	-0.02	-0.03
S	0.23	0.54	-0.24	-0.34
Sb	0.31	0.74	0.01	0.01
Sc INAA	-0.07	-0.16	-0.06	-0.09
Se	0.29	0.68	-0.15	-0.21
Sm INAA	-0.11	-0.27	-0.05	-0.07
Sr	0.10	0.24	-0.07	-0.10
Ta INAA	-0.04	-0.10	0.08	0.11
Tb INAA	-0.04	-0.10	0.23	0.33
Te	0.13	0.30	0.12	0.17
Th INAA	-0.13	-0.31	-0.01	-0.02
Ti	0.12	0.29	-0.31	-0.44
Tl	0.20	0.47	0.09	0.13
U INAA	0.19	0.45	-0.21	-0.30
V	0.17	0.40	-0.06	-0.08
W	0.04	0.10	-0.34	-0.48
Zn	0.25	0.60	0.07	0.11
Eigenvalues[2]	5.6		2.0	
Variation Score (%)[3]	12.3		4.3	

Notes:
[1]Contributions of input variables to the best-fit line or principal component.
[2]Variance of contributions within the principal component.
[3]Proportion of variance captured by the principal component.
[4]Loadings or lengths of the contributions from original variables scaled to the variance (eigenvalue) so that each principal component has a length of 1 (Fig. 14).
The input variables are log10-transformed and levelled values of original analytical determinations by inductively coupled plasma mass spectrometry or emission spectrometry and instrumental neutron activation analysis (INAA). The second and fourth principal components scores in the sediment samples are calculated as follows:

PC2 = -0.12*Eu - 0.031*Tb + 0.046*W + 0.11*Au + 0.29*Ag - 0.15*Al + 0.084*As - 0.22*Bi + 0.14*Br + 0.099*Ca + 0.38*Cd - 0.22*Ce - 0.041*Co + 0.0086*Cr + 0.14*Ba - 0.016*Cs + 0.27*Cu + 0.031*Fe - 0.14*Ga - 0.24*Hf + 0.27*Hg + 0.058*K - 0.19*La - 0.12*Lu + 0.017*Mg + 0.063*Mn + 0.40*Mo - 0.26*Na + 0.27*Ni + 0.23*P - 0.12*Pb - 0.097*Rb + 0.22*S + 0.44*Sb - 0.12*Sc + 0.34*Se - 0.22*Sm + 0.11*Sr - 0.018*Ta + 0.19*Te - 0.26*Th + 0.098*Ti + 0.25*Tl + 0.24*U + 0.277*V + 0.40*Zn + 1.1484.

PC4 = 0.26*Eu + 0.17*Tb - 0.36*W - 0.0068*Au + 0.19*Ag - 0.34*Al + 0.39*As - 0.042*Bi - 0.18*Br - 0.036*Ca + 0.060*Cd - 0.070*Ce - 0.020*Co + 0.025*Cr + 0.20*Ba + 0.020*Cs + 0.092*Cu + 0.061*Fe - 0.39*Ga - 0.014*Hf + 0.28*Hg - 0.11*K - 0.096*La - 0.030*Lu - 0.17*Mg + 0.050*Mn - 0.041*Mo - 0.71*Na + 0.077*Ni + 0.0034*P - 0.039*Pb - 0.021*Rb - 0.24*S + 0.013*Sb - 0.10*Sc - 0.18*Se - 0.10*Sm - 0.075*Sr + 0.034*Ta + 0.18*Te - 0.022*Th - 0.26*Ti + 0.12*Tl - 0.27*U - 0.087*V + 0.12*Zn + 0.6941.

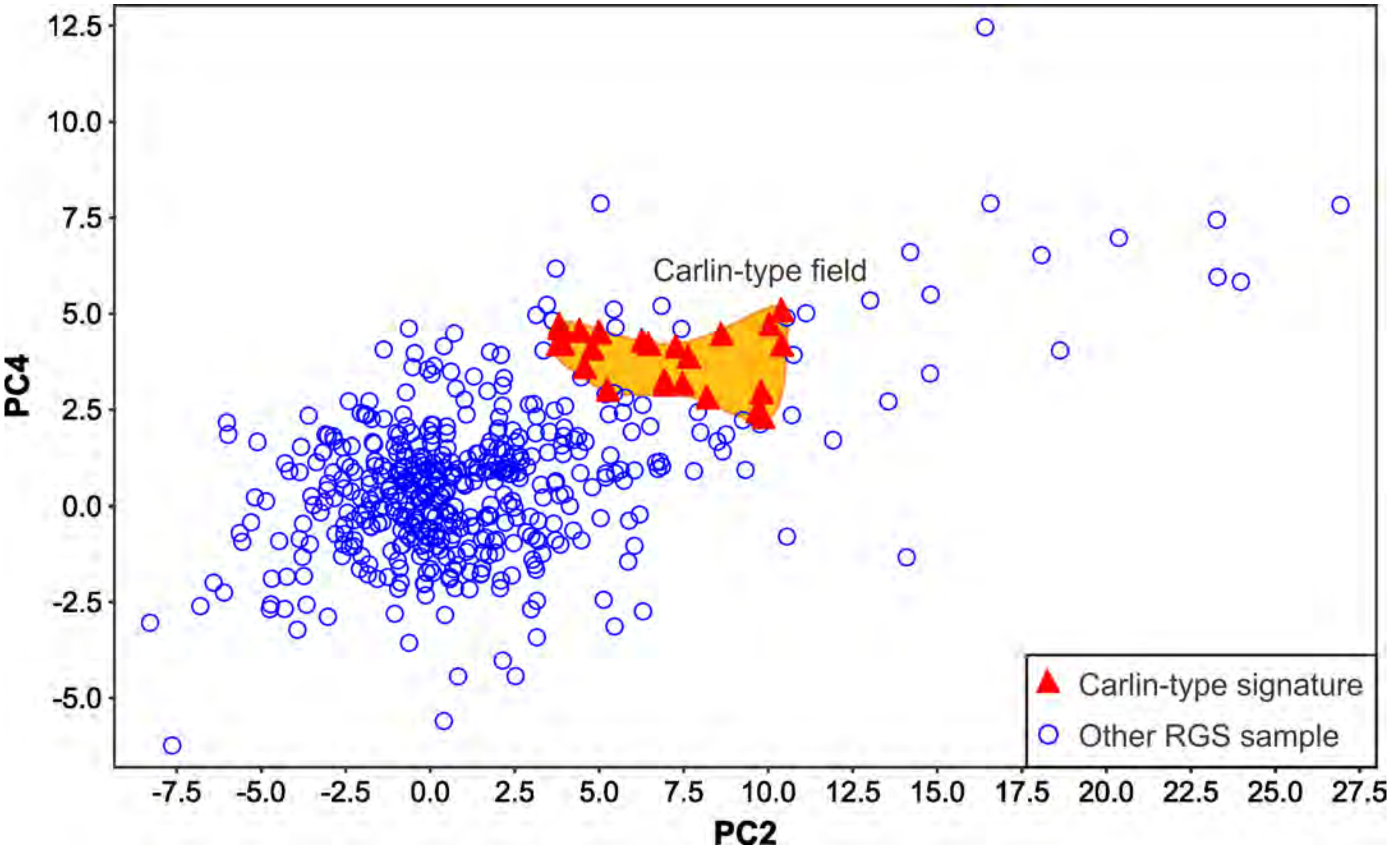

Fig. 11. Discrimination diagram showing Carlin-type field in terms of the second vs fourth principal components derived from the log-trasformed and levelled NGR and RGS data for lake and stream sediments from the Kechika trough and the Rackla belt using robustly estimated multi-element correlation matrix (Table 2). The PC2 and PC4 total to 16.6% of variation score in the original dataset (Table 3).

Table 4. Model parameters for weighted sum index of Carlin-type signal in the RGS/NGR lake- and stream-sediment samples from the Kechika trough, and the Rackla belt.

Element	W	Ag	As	Au	Ca	Fe	Hg	La	Sb	Sr	Te	Tl
Method[1]	ICPMS	ICPMS	ICPMS	ICPMS	ICPMS	INAA	ICPMS	INAA	ICPMS	ICPMS	ICPMS	ICPMS
Loading[2]	0.37	0.35	0.77	0.79	-0.14	0.31	0.85	-0.15	0.42	-0.18	0.58	0.83
Importance[3]	1	1	5	5	-1	1	5	-1	2	-1	3	5
Weight[3]	0.092	0.092	0.46	0.46	-0.092	0.092	0.46	-0.092	0.18	-0.092	0.27	0.46

Notes:
[1]ICPMS, aqua-regia extraction with inductively coupled plasma mass spectrometry finish; INAA, instrumental neutron activation analysis.
[2]Carlin-type Factor loadings derived from the factor analysis on >6,400 multi-element analyses of drill-core samples from the Jerritt Canyon district of CTGDs in Nevada (Patterson and Muntean, 2011).
[3]Assigned relative importance values and their weights are based on the Carlin-type factor loadings. See text for details.
The Carlin-type WS index score for each sample is calculated using the standardized analytical data on the stream and lake sediments as follows:

$$WS = 0.258*W + 0.0929*Ag + 0.469*As + 0.541*Au - 0.0972*Ca + 0.0948*Fe + 0.468*Hg - 0.0943*La + 0.187*Sb - 0.0937*Sr + 0.336*Te + 0.436*Tl + 0.0730.$$

stream- and lake-sediment samples from the Kechika trough (Fig. 17). Applied to stream sediments of the Rackla belt, these geochemical models consistently confirm the known Carlin-type occurrences in the area (Fig. 18), thus validating their effectiveness for evaluating Carlin-type potential. The stream and lake sediments with a Carlin-type signal contain up to 272 ppm As, 31 ppm Sb, 13.9 ppm Hg, 1.3 ppm Tl, 0.22 ppm Te, and 46 ppb Au (Rukhlov et al., 2014). The geochemical patterns and concentrations of pathfinder elements in these sediments are comparable to those of mineralized halos near the Carlin deposits in Nevada (Patterson and Muntean, 2011).

5. Kechika trough: highlights and conclusions

Regional stream- and lake-sediment geochemical surveys

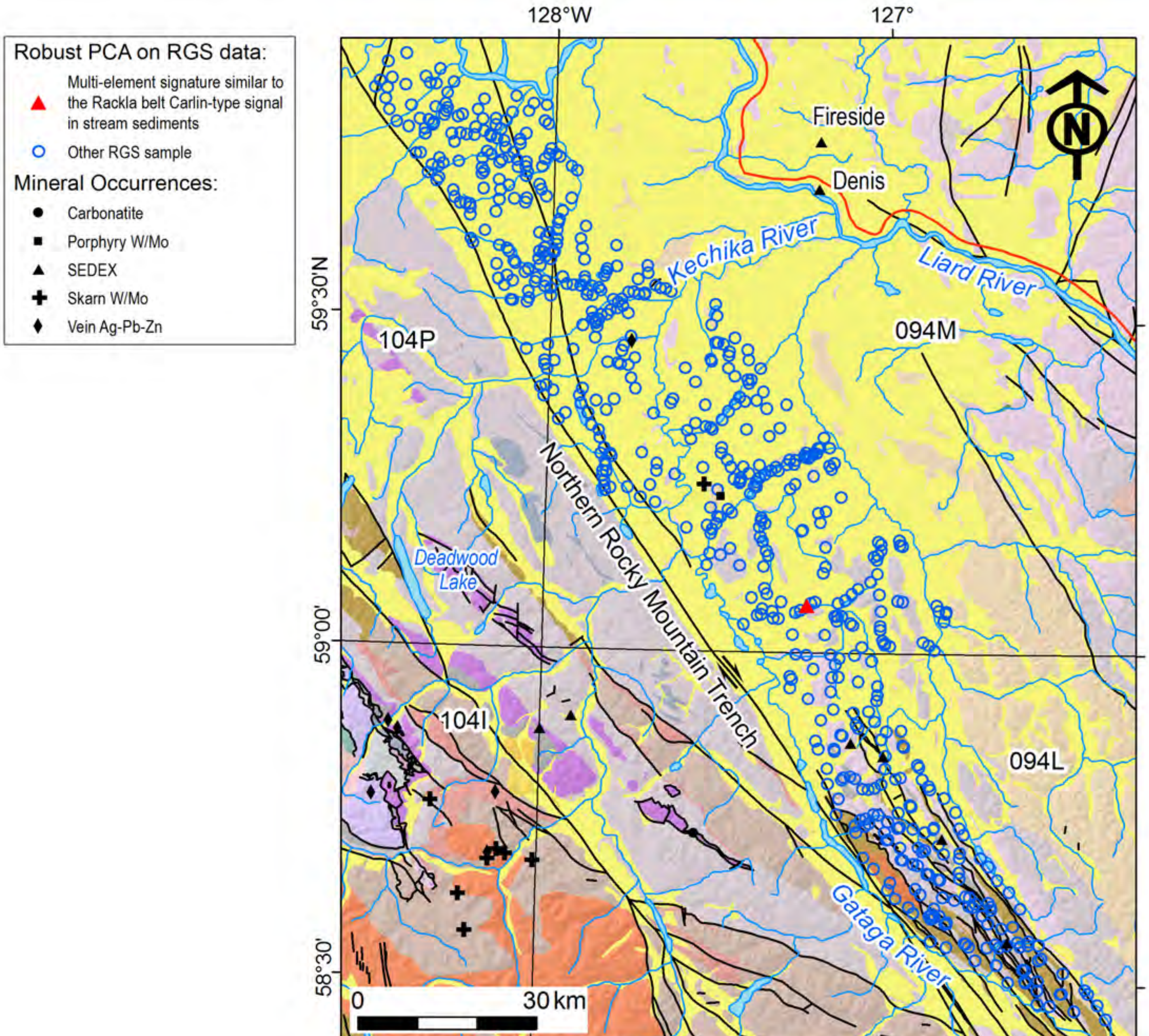

Fig. 12. Robust PCA on the RGS data, Kechika trough, highlighting multi-element Carlin-type signatures in samples with second and fourth principal component scores similar to those from the Rackla belt. Other symbols as in Figure 2.

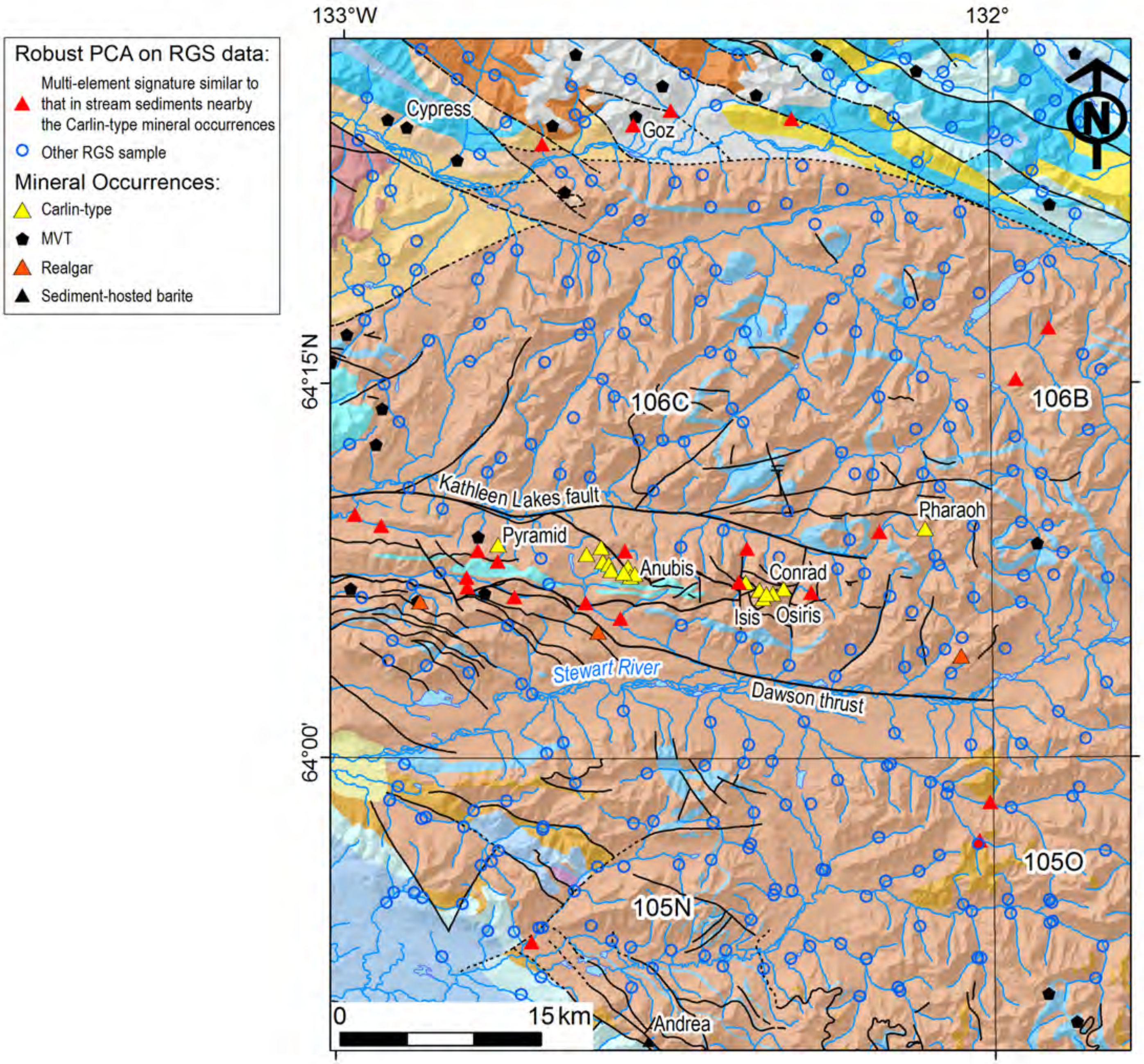

Fig. 13. Robust PCA on the NGR data, Rackla belt, highlighting multi-element Carlin-type signatures in samples with second and fourth principal component scores similar to those in samples nearby the Carlin-type mineral occurrences in the area. Rock legend as in Figure 3.

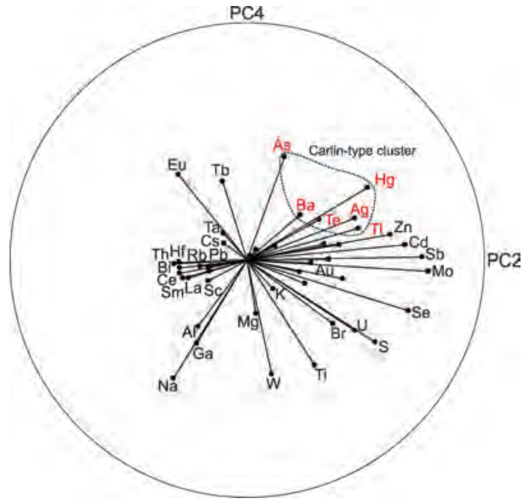

Fig. 14. Circle plot of scaled contributions (loadings) of each variable to PC2 and PC4 derived from robust PCA on the log10-trasformed and levelled RGS and NGR data for lake- and stream- sediments from the Kechika trough and the Rackla belt (Table 3). As, Hg, Tl, Te, Ba and Ag form a Carlin-type cluster (outlined). Analytes plotting closer to the unit circle (e.g., As, Hg and Tl) have higher loadings and are better represented by these components. Ca, Co, Cr, Cu, Fe, Lu, Mn, Ni, P, Sr, and V have relatively low loadings and are not labelled for clarity.

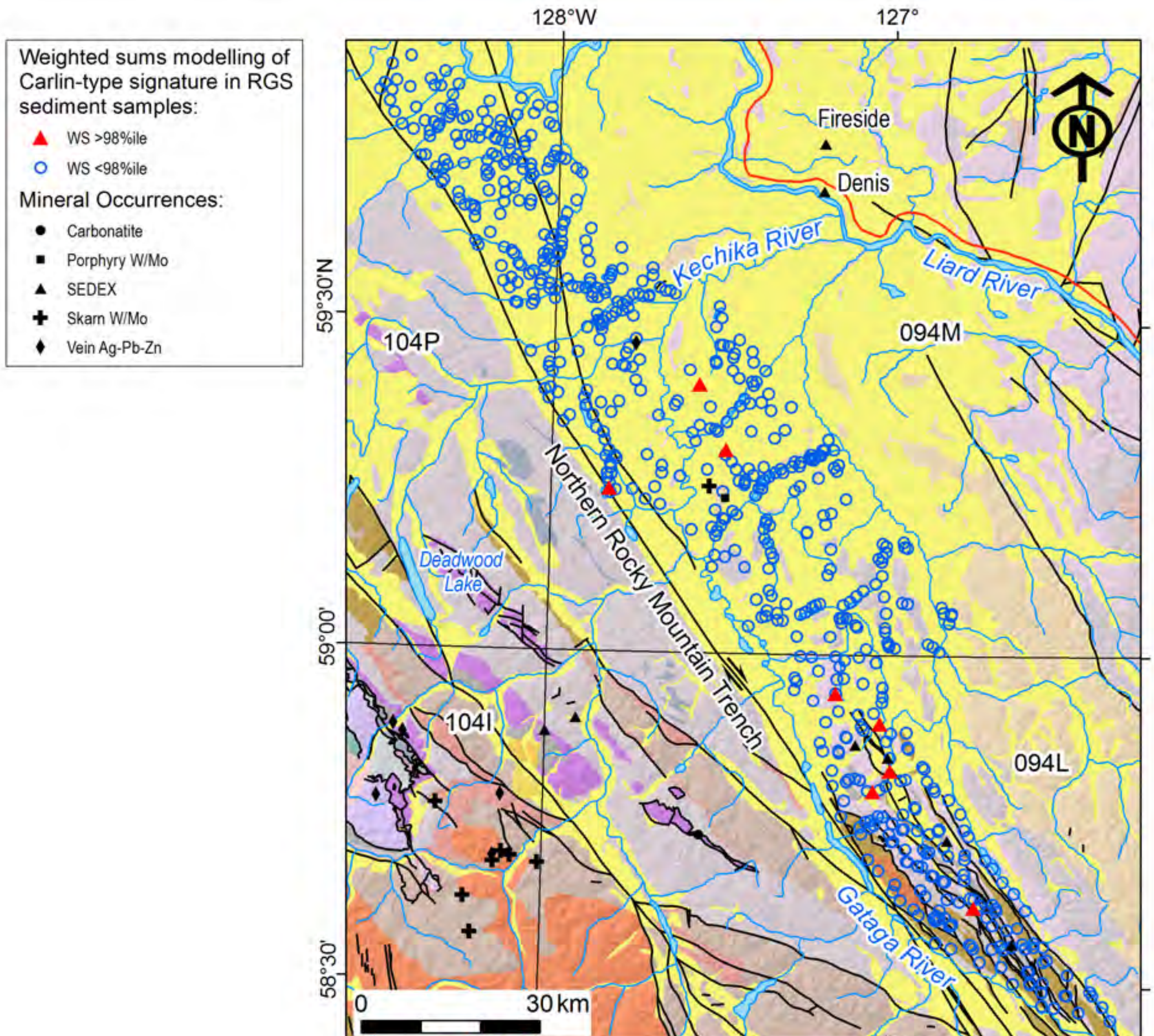

Fig. 15. Weighted sum index (WS) modelling of Carlin-type signature in the RGS sediments, Kechika trough (Table 4). Samples having the WS scores >98 percentile are highlighted. Rock legend as in Figure 2.

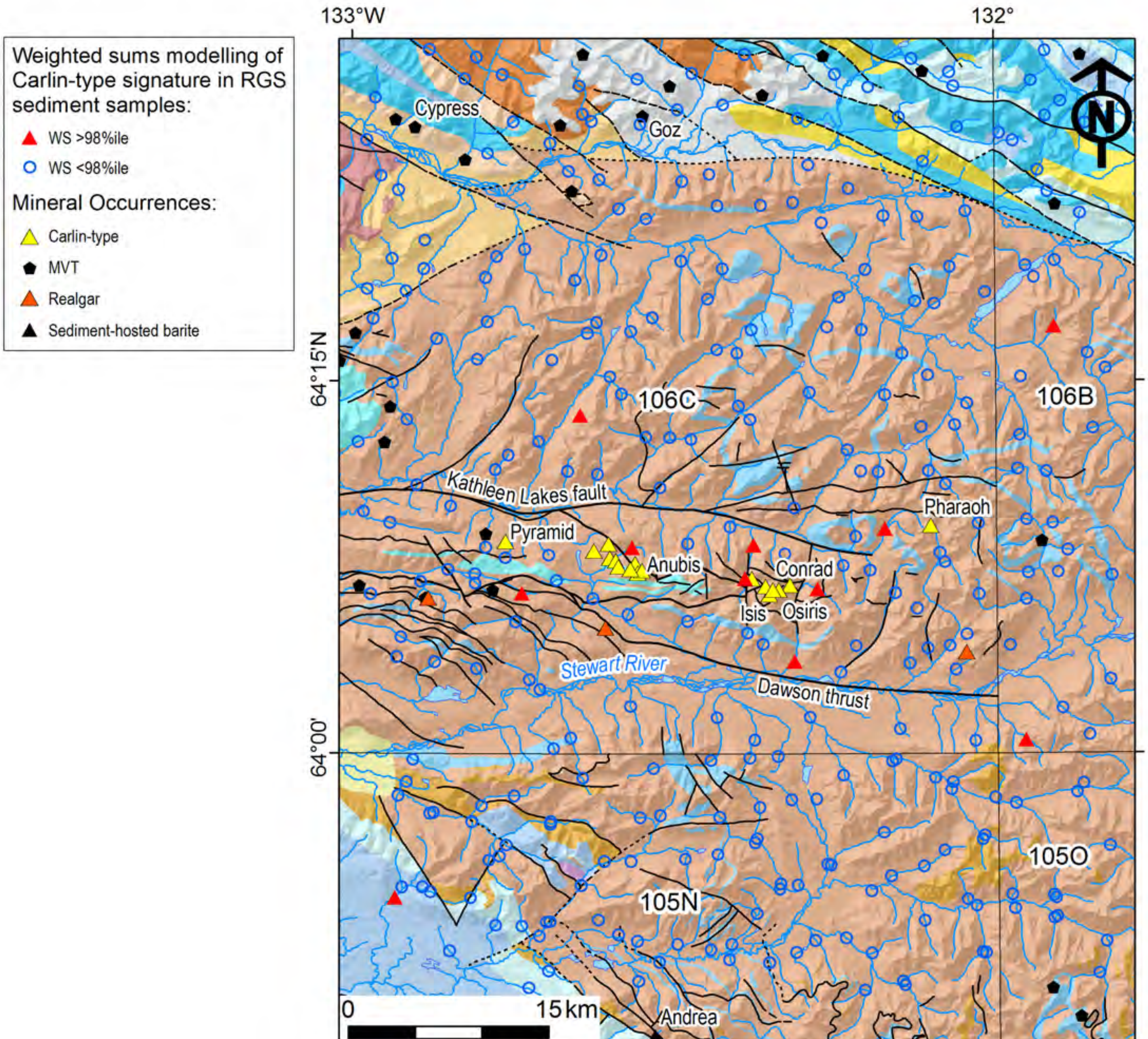

Fig. 16. Weighted sum index (WS) modelling of Carlin-type signature in the NGR stream sediments, Rackla belt. Samples having the WS scores >98 percentile (highlighted) predict the Carlin-type occurrences in the area. Rock legend as in Figure 3.

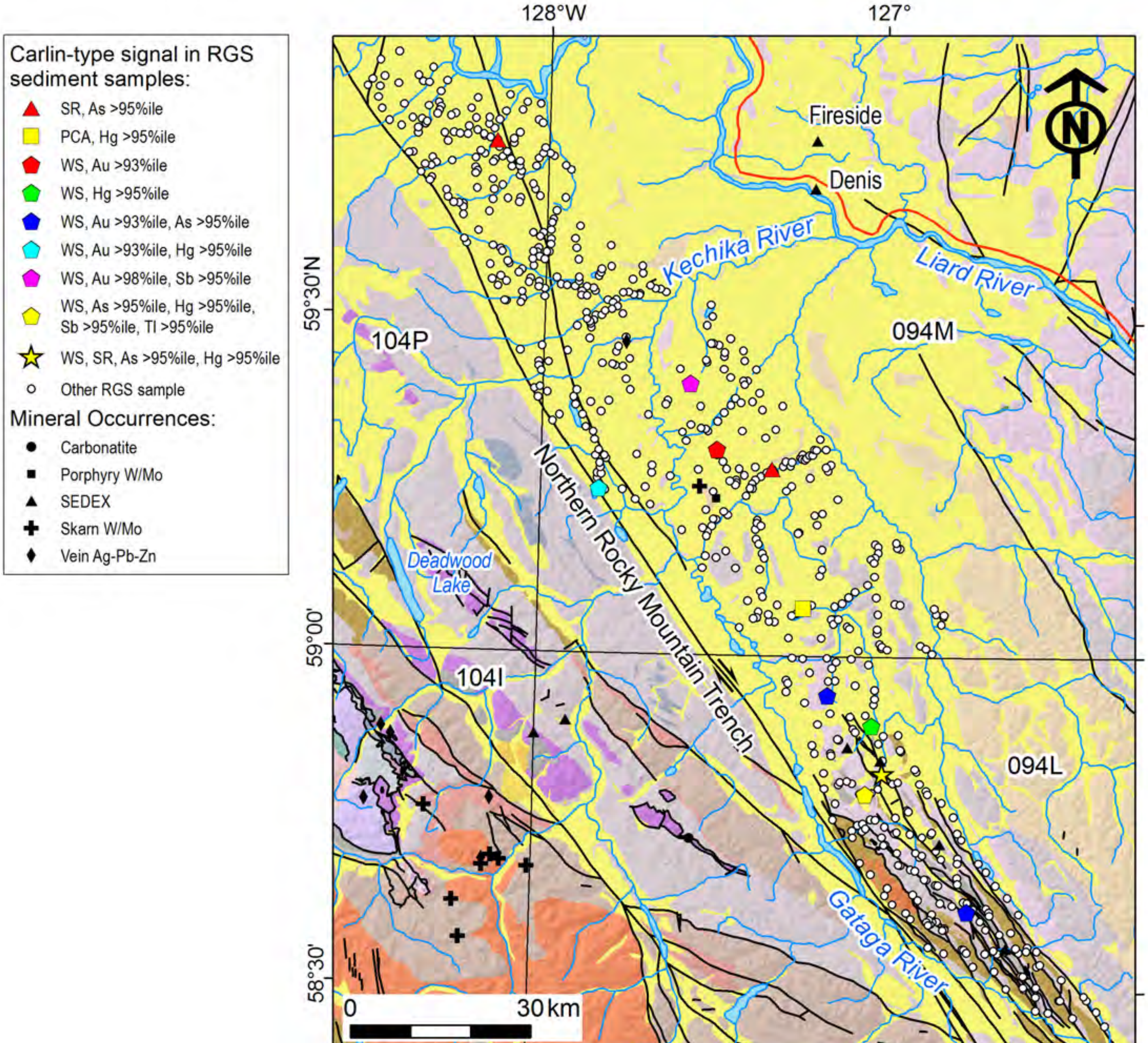

Fig. 17. RGS samples with interpreted Carlin-type signatures, Kechika trough (Appendix 4). Catchment basins for the anomalous stream-sediment samples are smaller than their map symbols. Rock legend as in Figure 2.

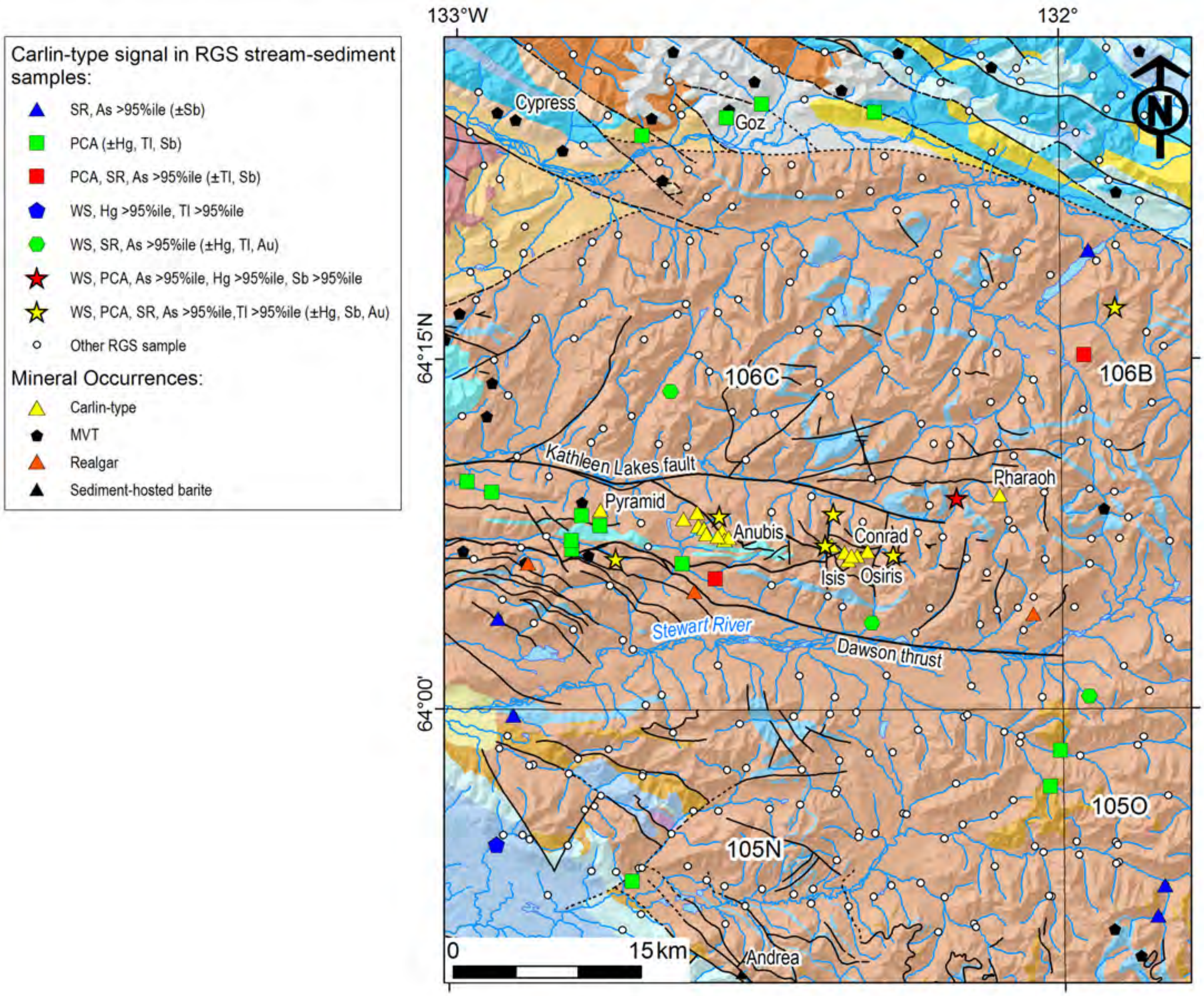

Fig. 18. NGR samples with interpreted Carlin-type signatures, Rackla belt (Appendix 4). Rock legend as in Figure 3.

can be used to identify areas that have potential for Carlin-type deposits (Tucker et al., 2013). Interpretation of raw analytical data is enhanced by standardization methods that normalize analyses, and by levelling procedures to account for sample medium, catchment basin size, and bedrock geology.

Coincident elevated concentrations of As±Hg±Tl±Sb±Au in sediments may be related to Carlin-style mineralization. However, because of nearby MVT, VMS-SEDEX, intrusion-related, and other types of base- and precious metal mineralization in the Kechika trough (Ferri et al., 1999) and the Rackla belt (Chakungal and Bennett, 2011) this interpretation is unclear.

Multi-element modelling of standardized RGS data using robust PCA and WS index scores and ‘indicator mineral’ regression analysis enhance the Carlin-type geochemical signal in sediments and independently confirm known Carlin-type deposits in the Rackla belt. Applied to the western flank of Kechika trough, these models highlight 11 lake and stream sediment samples that show the Carlin-type signatures (Fig. 17). These samples are underlain by fine-grained siliciclastic and carbonate rocks in the footwall of a thrust. South of the study area, Lett (2001) reported up to 147 ppb Au, 20 ppm As, 975 ppb Ag and 59 ppm Sb in black siliciclastic rocks of the Gunsteel Formation, north of the Bear mineral occurrence (NTS 094F 024). The elevated gold- and pathfinder-element bedrock anomalies, coupled with stratigraphic and structural similarities with the Rackla belt, suggest that Kechika trough holds potential for kindred Carlin-type deposits. The eastern margin of the Kechika trough has yet to be evaluated.

6. Exploration applications and future work

Carlin-type signals in low sample density stream and lake sediments mark new exploration targets in the Kechika trough. The Paleozoic and older fine-grained siliciclastic and carbonate rocks in this area also host numerous SEDEX Pb-Zn-Ba deposits and at least one known intrusion-related W-Mo stockwork-skarn deposit (e.g., Ferri et al., 1999). Exploration work might focus on bedrock and surficial geology mapping of the target catchment basins, complemented by geochemical surveys to locate favourable replacement and breccia zones near long-lived faults. Realgar, orpiment, and stibnite overprinting auriferous As-rich pyrite are the best indicators of Carlin-type mineralization (Tucker et al., 2013). However, exploration in the northern part of Kechika trough (parts of NTS 94M and 104P) has previously been limited by extensive drift cover and poor exposure. Drift prospecting and till geochemistry coupled with indicator mineralogy could aid interpretation of the geochemical anomalies.

Acknowledgments

We thank Yao Cui (British Columbia Geological Survey), Dani Alldrick (former British Columbia Geological Survey), and Maurice Colpron (Yukon Geological Survey) for useful comments. Thorough review by Larry Aspler (British Columbia Geological Survey) and Ray Lett (British Columbia Geological Survey) significantly improved this paper.

References

Arehart, G.B., 1996. Characteristics and origin of sediment-hosted disseminated gold deposits: a review. Ore Geology Reviews 11, 383-403.

Arehart, G.B., Ressel, M., Carne, R., Muntean, J., 2013. A comparison of Carlin-type deposits in Nevada and Yukon. In: Tectonics, Metallogeny, and Discovery: The North American Cordillera and Similar Accretionary Settings, M. Colpron, T. Bissig, B.G. Rusk, and J.F.H. Thompson (eds.), Society of Economic Geologists, Inc., Special Publication 17, pp. 389–401.

ATAC Resources Ltd., 2010. ATAC Resources Makes a New Gold Discovery On its Rau Gold Project - Yukon. July 29, 2010. Accessed online from ATAC Resources Ltd. (http://www.atacresources.com/s/NewsReleases.asp?), October 07, 2014.

Blusson, S.L., 1974. Five geological maps of northern Selwyn Basin (Operation Stewart), Yukon Territory and District of Mackenzie, N.W.T. Geological Survey of Canada, Open File 205.

Bonham-Carter, G.F., Goodfellow, W.D., 1986. Background corrections to stream geochemical data using digitized drainage and geological maps: Application to Selwyn Basin, Yukon and Northwest Territories. In: Exploration for ore deposits of the North American Cordillera, C.E. Nichols (ed.). Journal of Geochemical Exploration 25 (1-2), p. 139–155.

Campbell, N.A., 1980. Robust procedures in multivariate analysis. I: Robust covariance estimation. Applied Statistics 29, 231–237.

Chakungal, J., Bennett, V., 2011. New bedrock geology of Mount Mervyn map sheet (106C/04) and mineral potential for the South Wernecke mapping project. In: Yukon Exploration and Geology 2010, K.E. MacFarlane , L.H. Weston and C. Relf (eds.), Yukon Geological Survey, p. 55-87.

Colpron, M., 2012. Preliminary geological map of the Mount Ferrell area (106C/3), central Yukon. Yukon Geological Survey, Open File 2012-11, 1:50 000 scale.

Colpron, M., Moynihan, D., Israel, S., Abbott, G., 2013. Geological map of the Rackla belt, east-central Yukon (NTS 106C/1-4, 106D/1). Yukon Geological Survey, Open File 2013-13, 1:50 000 scale.

Cook, S.J., Jackaman, W., Friske, P.W., Day, S.J., Coneys, A.M., Ferri, F., 1997. Regional lake sediment and water geochemistry of the northern Kechika Trough, British Columbia (NTS 94M/2, 3, 4, 5, 6, 12; 104P/8, 9, 10, 15, 16). British Columbia Ministry of Employment and Investment, British Columbia Geological Survey Open File 1997-15, Geological Survey of Canada Open File 3499, 31 p.

Cook, J., Jackaman, W., Friske, P.W., Day, S.J., Hall, G.E.M., Coneys, A.M., 1999. Geochemistry of Alkaline Lake Waters of the Northern Kechika Trough, British Columbia (NTS 94M/2, 3, 4, 5, 6, 12; 104P/8, 9, 10, 15, 16). British Columbia Ministry of Energy and Mines, British Columbia Geological Survey Open File 1999-6, Geological Survey of Canada Open File 3704, 47 p.

Cui, Y., Katay, F., Nelson, J.L., Han, T., Desjardins, P.J., Sinclair, L., compilers, 2013. British Columbia Digital Geology. British Columbia Ministry of Energy and Mines, British Columbia Geological Survey, Open File 2013-4.

Day, S.J.A., McCurdy, M.W., Friske, P.W.B., McNeil, R.J., Hornbrook, E.H.W., Lynch, J.J., Durham, C.C., Gross, H., Galletta, A.C., 2009. Regional stream sediment and water geochemical data, Lansing Range area, east central Yukon (NTS 105N). Geological Survey of Canada, Open File 6272, Yukon Geological Survey, Open File 2009-27, 11 p.

Ferri, F., Rees, C., Nelson, J., Legun, A., 1999. Geology and mineral deposits of the northern Kechika trough between Gataga River and the 60th parallel. British Columbia Ministry of Energy and Mines, British Columbia Geological Survey Bulletin 107, 122 p.

Fletcher, W.K., 1997. Stream sediment geochemistry in today's exploration world. In: Geophysics and Geochemistry at the Millenium. Proceedings of Exploration 97: Fourth Decennial International Conference on Mineral Exploration, A.G. Gubbins (ed.), Prospectors and Developers Association of Canada, p. 249-260.

Friske, P.W.B., Hornbrook, E.H.W., 1991. Canada's National Geochemical Reconnaissance programme. Transactions of the Institution of Mining and Metallurgy, London, Section B 100, 47–56.

Friske, P.W.B., Hornbrook, E.H.W., Lynch, J.J., McCurdy, M.W., Gross, H., Galletta, A.C., Durham, C.C., 1991a. National Geochemical Reconnaissance stream sediment and water data, east central Yukon (NTS 105N). Geological Survey of Canada, Open File 2363, 140 p.

Friske, P.W.B., Hornbrook, E.H.W., Lynch, J.J., McCurdy, M.W., Gross, H., Galletta, A.C., Durham, C.C. 1991b. National Geochemical Reconnaissance stream sediment and water data, east central Yukon (NTS 105O; parts of 105P). Geological Survey of Canada, Open File 2364, 140 p.

Gabrielse, H., 1962. Kechika map area. Geological Survey of Canada, Preliminary Map 42-1962, 1:253,440 scale.

Gabrielse, H., 1963a. Rabbit River map area. Geological Survey of Canada, Preliminary Map 46-1962, 1:253,440 scale.

Gabrielse, H., 1963b. McDame map area, Cassiar District, British Columbia. Geological Survey of Canada, Memoir 319, 138 p.

Gabrielse, H., 1998. Geology of Cry Lake and Dease Lake map areas, north-central British Columbia. Geological Survey of Canada, Bulletin 504, 147 p.

Garrett, R.G., Grunsky, E.C., 2001. Weighted sums - knowledge based empirical indices for use in exploration geochemistry. Geochemistry: Exploration, Environment, Analysis 1, 135–141.

Gordey, S.P., Makepeace, A.J., compilers, 1999. Yukon bedrock geology in Yukon digital geology. Geological Survey of Canada, Open File D3826/ Indian and Northern Affairs Canada, Exploration and Geological Services Division, Yukon, Open File 1999-1(D).

Grunsky, E.C. 2007. The interpretation of regional geochemical survey data. In: Advances in Regional-Scale Geochemical Methods, Proceedings of Exploration 07: Fifth Decennial International Conference on Mineral Exploration, B. Milkereit (ed.), Geological Survey of Canada, Paper 8, p. 139–182.

Hart, J.R., Mair, J.L., Goldfarb, J.R., Groves, I.G., 2004. Source and redox controls on metallogenic variations in intrusion-related ore systems, Tombstone-Tungsten Belt, Yukon Territory, Canada. Transactions of the Royal Society of Edinburgh. Earth Sciences 95, 339–356.

Heberlein, D.R., 2013. Catchment basin analysis and weighted sums modelling: enhanced interpretation of RGS data using examples from map sheets NTS 105M, 105O and part of 105P. Yukon Geological Survey, Open File 2013-16, 18 p.

Héon, D., compiler, 2003. Yukon Regional Geochemical Database 2003 - Stream sediment analyses. Exploration and Geological Services Division, Yukon Region, Indian and Northern Affairs Canada.

Hawkes, H.E., 1976. The downstream dilution of stream sediment anomalies. Journal of Geochemical Exploration 6, p. 345–358.

Jackaman, W., Lett, R., Sibbick, S., 1996. Geochemistry of the Gataga Mountain area. British Columbia Ministry of Employment and Investment, British Columbia Geological Survey Open File 1996-18, 194 p.

Jackaman, W., 2011a. Northern BC Sample Reanalysis Project. Geoscience BC, Report 2011-2, 11 p.

Jackaman, W., 2011b. Regional stream sediment geochemical data Niddery Lake, Yukon (105O & P). Yukon Geological Survey, Open File 2011-30, 116 p.

Lett, R., 2001. Geochemical exploration models Vol 2: Shale hosted Pb-Zn-Ag deposits in NE BC (94F/13, 94K/4 and 94L/1). British Columbia Ministry of Energy, Mines and Petroleum Resources, British Columbia Geological Survey Open File 2001-07, 74 p.

Lett, R., Jackaman, W., Sibbick, S., 1996. Spring water and spring sediment geochemistry of the Gataga Mountain area (parts of 94L/7, 8, 9, 10, 11, 14, 15). British Columbia Ministry of Employment and Investment, British Columbia Geological Survey Open File 1996-30, 27 p.

Muntean, J. L., Cline, J. S., Simon, A. C., Anthony, A. L., 2011. Magmatic-hydrothermal origin of Nevada's Carlin-type gold deposits. Nature Geoscience 4, 122–127.

Patterson, L.M., Muntean, J.L., 2011. Multi-element geochemistry across a Carlin-type gold district: Jerritt Canyon, Nevada. In: Great Basin Evolution and Metallogeny, R. Steininger and B. Pennell (eds.), Geological Society of Nevada 2010 Symposium, Reno, NV, United States, DEStech Publications, Lancaster, PA, United States, p.1119–1151.

Poulsen, K. H., 1996. Carlin-type gold deposits and their potential occurrence in the Canadian Cordillera. In: Geological Survey of Canada, Current Research 1996-A, p.1–9.

Rock, N.M.S., 1988. Numerical Geology: A Source Guide, Glossary and Selective Bibliography to Geological Uses of Computers and Statistics. Lecture Notes in Earth Sciences 18, Springer-Verlag, Berlin, 427 p.

Rousseeuw, P.J., Leroy, A.M., 1987. Robust Regression and Outlier Detection. Series in Applied Probability and Statistics, Wiley-Interscience, New York, 329 p.

Rukhlov, A.S., Han, T., Nelson, J., Hickin, A., Ferri, F., 2014. Supplementary data for Carlin-type geochemical signal in lake and stream sediments from Kechika trough, north-central British Columbia. British Columbia Ministry of Energy and Mines, British Columbia Geological Survey GeoFile 2014-10.

Thiessen, E.J., Gleeson, S.A., Dufrane, S.A., Carne, R.C., Dumala, M., 2012. Upper age constraint and paragenesis of the Tiger zone, Rau property, central Yukon. In: Yukon Exploration and Geology 2011, K.E. MacFarlane and P.J. Sack (eds.), Yukon GeologicalSurvey, p. 151–164.

Tucker, M.J., Hart, C.J.R., Carne, R.C., 2013. Geology, alteration, and mineralization of the Carlin-type Conrad zone, Yukon. In: Yukon Exploration and Geology 2012, K.E. MacFarlane, M.G. Nordling, and P.J. Sack (eds.), Yukon Geological Survey, p.163–178.